# Journal of Visualized Experiments

## Location, Dissection, and Analysis of the Murine Stellate Ganglion

--Manuscript Draft--

| | |
|---|---|
| **Article Type:** | Invited Methods Collection - JoVE Produced Video |
| **Manuscript Number:** | JoVE62026R1 |
| **Full Title:** | Location, Dissection, and Analysis of the Murine Stellate Ganglion |
| **Corresponding Author:** | Katharina Scherschel<br><br>GERMANY |
| **Corresponding Author's Institution:** | |
| **Corresponding Author E-Mail:** | katharina.scherschel@evk-duesseldorf.de |
| **Order of Authors:** | Katharina Scherschel |
| | Hanna Bräuninger |
| | Klara Glufke |
| | Christiane Jungen |
| | Nikolaj Klöcker |
| | Christian Meyer |
| **Additional Information:** | |
| **Question** | **Response** |
| Please specify the section of the submitted manuscript. | Medicine |
| Please indicate whether this article will be Standard Access or Open Access. | Open Access (US$4,200) |
| Please indicate the **city, state/province, and country** where this article will be **filmed**. Please do not use abbreviations. | Düsseldorf, Germany |
| Please confirm that you have read and agree to the terms and conditions of the author license agreement that applies below: | I agree to the Author License Agreement |
| Please provide any comments to the journal here. | |

**TITLE:**

# Location, Dissection, and Analysis of the Murine Stellate Ganglion

**AUTHORS AND AFFILIATIONS:**

Katharina Scherschel[1,2,3], Hanna Bräuninger[3,4], Klara Glufke[2], Christiane Jungen[2,4,5], Nikolaj Klöcker[3], Christian Meyer[1,2,3]

[1]Division of Cardiology, EVK Düsseldorf, cNEP, cardiac Neuro- and Electrophysiology Re-search Consortium, Kirchfeldstrasse 40, 40217 Düsseldorf, Germany

[2]DZHK (German Centre for Cardiovascular Research), Partner Site Hamburg/Kiel/Lübeck, Germany

[3]Institute of Neural and Sensory Physiology, Medical Faculty, Heinrich Heine University Düsseldorf, Universitätsstrasse 1, 40225 Düsseldorf, Germany

[4]Clinic for Cardiology, University Heart & Vascular Centre, University Hospital Hamburg-Eppendorf, Martinistrasse 52, 20246 Hamburg, Germany

[5]Department of Cardiology, Leiden University Medical Center, Leiden, the Netherlands

Email Addresses of Co-Authors:

Katharina Scherschel (katharina.scherschel@hhu.de)
Hanna Bräuninger (h.braeuninger@uke.de)
Klara Glufke (klara.glufke@stud.uke.uni-hamburg.de)
Christiane Jungen (c.jungen@lumc.nl)
Nikolaj Klöcker (nikolaj.kloecker@uni-duesseldorf.de)
Christian Meyer (christian.meyer@evk-duesseldorf.de)

Corresponding Author:

Christian Meyer (christian.meyer@evk-duesseldorf.de)

**KEYWORDS:**

sympathetic nervous system, stellate ganglia, intracardiac autonomic nervous system, ventricular arrhythmia, neuromorphology, electrophysiology

**SUMMARY:**

Pathophysiological changes in the cardiac autonomic nervous system, especially in its sympathetic branch, contribute to the onset and maintenance of ventricular arrhythmias. In the present protocol, we show how to characterize murine stellate ganglia to improve the understanding of the underlying molecular and cellular processes.

**ABSTRACT:**

The autonomic nervous system is a substantial driver of cardiac electrophysiology. Especially, the role of its sympathetic branch is an ongoing matter of investigation in the pathophysiology of ventricular arrhythmias (VA). Neurons in the stellate ganglia (SG)—bilateral star-shaped structures of the sympathetic chain—are an important component of the sympathetic infrastructure. The SG are a recognized target for the treatment via cardiac sympathetic denervation in patients

with therapy-refractory VA. While neuronal remodeling and glial activation in the SG have been described in patients with VA, the underlying cellular and molecular processes that potentially precede the onset of arrhythmia are only insufficiently understood and should be elucidated to improve autonomic modulation. Mouse models allow us to study sympathetic neuronal remodeling, but identification of the murine SG is challenging for the inexperienced investigator. Thus, in-depth cellular and molecular biological studies of the murine SG are lacking for many common cardiac diseases. Here, we describe a basic repertoire for dissecting and studying the SG in adult mice for analyses at RNA level (RNA isolation for gene expression analyses, in situ hybridization), protein level (immunofluorescent whole mount staining), and cellular level (basic morphology, cell size measurement). We present potential solutions to overcome challenges in the preparation technique, and how to improve staining via quenching of autofluorescence. This allows for the visualization of neurons as well as glial cells via established markers in order to determine cell composition and remodeling processes. The methods presented here allow characterizing the SG to gain further information on autonomic dysfunction in mice prone to VA and can be complemented by additional techniques investigating neuronal and glial components of the autonomic nervous system in the heart.

**INTRODUCTION:**

The cardiac autonomic nervous system is a tightly regulated equilibrium of sympathetic, parasympathetic, and sensory components that allows the heart to adapt to environmental changes with the appropriate physiological response[1,2]. Disturbances in this equilibrium, for example, an increase of sympathetic activity, have been established as a key driver for the onset as well as maintenance of ventricular arrhythmias (VA)[3,4]. Therefore, autonomic modulation, achieved via pharmacological reduction of sympathetic activity with beta-blockers, has been a cornerstone in the treatment of patients with VA for decades[5,6]. But despite pharmacological and catheter-based interventions, a relevant number of patients still suffers from recurrent VA[7].

Sympathetic input to the heart is mostly mediated via neuronal cell bodies in the stellate ganglia (SG), bilateral star-shaped structures of the sympathetic chain, which relay information via numerous intrathoracic nerves from the brainstem to the heart[8–10]. Nerve sprouting from the SG after injury is associated with VA and sudden cardiac death[11,12], emphasizing the SG as a target for autonomic modulation[13,14]. A reduction of sympathetic input to the heart can be achieved temporarily via percutaneous injection of local anesthetics or permanently by partial removal of the SG via video-assisted thoracoscopy[15,16]. Cardiac sympathetic denervation presents an option for patients with therapy-refractory VA with promising results[14,16,17]. We have learned from explanted SG of these patients that neuronal and neurochemical remodeling, neuro-inflammation and glial activation are hallmarks of sympathetic remodeling that might contribute or aggravate autonomic dysfunction[18,19]. Still, the underlying cellular and molecular processes in these neurons remain obscure to date, for example, the role of neuronal transdifferentiation into a cholinergic phenotype[20,21]. Experimental studies present novel approaches to treat VA, for example, the reduction of sympathetic nerve activity via optogenetics[22], but in-depth characterization of the SG is still lacking in many cardiac pathologies that go in hand with VA. Mouse models mimicking these pathologies allow to study neuronal remodeling that potentially precedes the onset of arrhythmias[12,23]. These can be completed by further morphological and functional analyses for

autonomic characterization of the heart and the nervous system. In the present protocol, we provide a basic repertoire of methods allowing to dissect and characterize the murine SG to improve the understanding of VA.

**PROTOCOL:**

All procedures involving animals were approved by the Animal Care and Use Committee of the State of Hamburg (ORG870, 959) and conform to the National Institutes of Health's Guide for the Care and Use of Laboratory Animals (2011). Studies were performed using male and female (aged 10–24 weeks) C57BL/6 mice (stock number 000664, Jackson Laboratories) and mice homozygous (db/db) or heterozygous (db/het; control) for the diabetes spontaneous mutation ($Lepr^{db}$; BKS.Cg-$Dock7^{m+/+}$ Leprdb /J, stock number 000642, Jackson Laboratories). The authors have used the protocols at hand without variations for mice aged up to 60 weeks.

## 1. Location and dissection of murine stellate ganglia

NOTE: Even though descriptions and drawings are mostly available in bigger species, some publications have previously described the location of the SG in rats[24] and mice[25] using anatomical methods and fluorescent reporter lines, respectively.

1.1. Prepare 50 mL of ice-cold (3–4 °C) heparinized (20 units/mL, see **Table of Materials**) phosphate-buffered saline (PBS). Perform dissection of the SG at room temperature (RT).

1.2. Deeply anesthetize mouse by inhalation of 3%–5% isoflurane according to the institutional and local guidelines. Verify adequate anesthesia by loss of pedal withdrawal reflex. Decapitate mice or perform cervical dislocation.

NOTE: Incorrect cervical dislocation can result in breakage of the spine and damage of thoracic vessels leading to bleeding which hinders in the preparation or the severing of the sympathetic chain, so that SG are not in their correct position. Therefore, it is critical to have experienced personnel perform cervical dislocation or decapitate animals in deep sedation.

1.3. Spray the skin with ethanol and open the thorax with two incisions along the anterior axillary lines using Mayo scissors and narrow pattern forceps. Cut the diaphragm and remove the complete ribcage.

1.4. Remove the heart-lung package by gripping the aorta and vena cava right above the diaphragm using London forceps and cutting all vessels and connective tissue close to the spine below with the Strabismus scissors.

1.5. Flush the thorax thoroughly with heparinized PBS using a plastic disposable pipette until all traces of blood are removed.

1.6. Place the torso under stereomicroscope preparation binoculars and ensure good lighting in the thorax with external light sources.

1.7. Locate the first rib and the longus colli muscles.

NOTE: The SG are located bilaterally, parallel to the spine at the branch between the first rib and the spine, in a groove lateral to the longus colli muscles[24]. The flat side of the SG is located adjacent to the longus colli muscles. Depending on the preparation, parts of the sympathetic chain might already be visible as white, oblique fibers parallel to the spine. These can be traced along to the SG.

1.8. Gently use the tip of the Dumont #5/45 forceps to expose the connective tissue lateral to the longus colli muscle.

1.9. Turn the forceps around by 180° and use the flat side to grip the SG and pull it out with minimal pressure.

1.10. Repeat with the second SG.

1.11. Place both SG in a dish (6 cm diameter) filled with cold PBS and inspect with the appropriate magnification. If necessary, remove excess vessels, fat tissue, and larger nerves.

NOTE: Autonomic ganglia are surrounded by a connective tissue capsule consisting of collagen fibers and fibroblasts[26,27]. The permeability of these capsules seems to vary among species, different kind of ganglia[26] and age[28]. Remove as much connective tissue as possible using Dumont #5/45 forceps and, if necessary, spring scissors. Depending on the goal of the experiment, proceed with section 2, 3, or 4 of this protocol.

## 2. Whole mount immunohistochemistry protocol

NOTE: This protocol is adapted from cardiac whole mount stainings[4,29]. Perform incubation steps for every single SG in one well of a 96-well plate and use 100 µL (for antibody-containing solutions) to 200 µL (for all other solutions) of the solution to ensure complete coverage. Regularly check the coverage and correct immersion of the SG with binoculars. Remove liquids manually with a 200 µL pipette with an additional 10 µL tip on top of the 200 µL tip. This will prevent aspiration of the SG in the pipette tip. Use freshly prepared solutions and sterile liquids to prevent bacterial growth.

2.2. Fix SG for histology for 2 h at RT in 4% methanol-free paraformaldehyde (PFA)/PBS.

2.3. Process SG as quickly as possible, but they can be stored for 2–4 weeks at 4–6 °C in PBS with 0.02% (w/v) sodium azide at this point.

2.4. Prepare Sudan black stock solution (1% Sudan black w/v in 100% ethanol) for reduction of autofluorescence and improvement of signal to background ratio[30]. Dissolve for 2–3 h on a magnetic stirrer at RT.

NOTE: Use the stock solution for a maximum of 6–8 weeks, discard earlier when sedimentation appears.

2.5. Prepare Sudan black working solution by centrifuging the stock solution for 30 min at full speed (13,000 x *g*) to remove debris and diluting the stock in 70% ethanol to a final concentration of 0.25% Sudan black.

2.6. Treat SG with Dent's bleach to improve antibody permeabilization[31]. Freshly prepare Dent's bleach by mixing methanol (MeOH), hydrogen peroxide solution 30% (w/w) in $H_2O$ and dimethyl sulfoxide (DMSO) in a ratio of 4:1:1. Add 200 µL per SG and place the plate on an orbital shaker for 1 h at RT.

2.7. Perform a descending MeOH series for rehydration by incubating for 10 min each on an orbital shaker: 100% MeOH, 75% MeOH/PBS, 50% MeOH/PBS, 25% MeOH/PBS.

2.8. Perform permeabilization by incubating SG twice for 60 min each in PBS/1% Triton-X-100 at RT.

2.9. Remove permeabilization solution from the SG and add Sudan black working solution. Incubate for 2 h at RT on an orbital shaker.

2.10. In the meantime, prepare a blocking solution by adding 5% receptor grade bovine serum albumin (BSA) and 0.1% Triton-X-100 in PBS a 15 mL vessel and let it dissolve on a roller shaker for approximately 5–10 min. Decant through a pre-pleated paper filter to remove debris.

2.11. Remove Sudan black very carefully by tilting the plate and carefully pipetting from the upright side.

NOTE: It is not possible to see the SG in Sudan black. Use a strong light source and work slowly. From this step on, SG are stained black, enhancing visualization. If any additional connective tissue is seen surrounding SG at this point, remove it using Dumont #5/45 forceps and spring scissors.

2.12. Add 200 µL of PBS/0.1% Triton-X-100 (PBS-T) and wash for 5 min at RT on an orbital shaker.

2.13. Remove PBS-T by aspirating it with a pipette and repeat 2 times.

2.14. Remove PBS; add 200 µL of blocking solution and incubate at 4 °C overnight on an orbital shaker.

2.15. On the next day, prepare solutions by adding primary antibodies in the blocking solution. Adapt antibody concentrations from established protocols.

NOTE: Include one SG as antibody control without primary antibody (incubated with antigen-preabsorbed antibody or IgG, if available, or blocking buffer).

2.16. Perform primary antibody incubation for 36–48 h at 4 °C on an orbital shaker. For cell size measurements and staining of sympathetic neurons, use antibodies against tyrosine hydroxylase (see **Table of Materials** for antibody recommendations).

NOTE: Place the 96-well plate in a wet chamber (e.g., plastic box lined with dd$H_2O$-wetted paper towels) to prevent evaporation at this point.

2.17. Remove antibody solution carefully and add 200 µL of PBS-T. Place the plate on an orbital shaker for 30 min.

2.18. Remove PBS-T and repeat the washing step 5 additional times.

2.19. Prepare the secondary antibody working solution by centrifuging fluorescent Alexa-labeled secondary antibodies for 1 min at full speed (13,000 x *g*) before usage. Dilute the appropriate secondary antibodies according to the primary antibodies 1:500 in the blocking solution and add to SG. Add 1 µg/mL of bisbenzimide H33342 trihydrochloride (Hoechst staining) if nuclear staining is desired. Incubate for 12–24 h at 4 °C on an orbital shaker.

2.20. Remove the antibody solution carefully and add 200 µL of PBS-T. Place the plate on an orbital shaker for 30 min.

2.21. Remove PBS-T and repeat the washing step 5 additional times. For the last step, use PBS without Triton.

2.22. For embedding, spread 50–100 µL of fluorescent mounting medium (see **Table of Materials**) on a glass slide and place under preparation binoculars. Use Dumont #5/45 forceps to pick up SG from the 96-well plate and remove excess liquid by dipping one end on a filter paper (e.g., Whatman drying pad) and place it on the drop.

2.23. Use Dumont #5/45 forceps to correct positioning with the appropriate magnification.

2.24. Gently place a glass coverslip (20 mm x 20 mm) next to the SG and slowly descend.

NOTE: Using too much mounting medium will result in movement of the SG or tangling of nerves. If that happens, quickly remove the coverslip and repeat steps 2.9–2.21.

2.25. Let the slides dry in the dark overnight at RT. Storage of the stained specimen is possible for at least 4–6 weeks at 4 °C.

## 3. Whole mount in situ hybridization

NOTE: Whole-mount in situ-hybridization of the SG is adapted from the organ of corti[32] and the commercial RNA fluorescence in situ protocol (see **Table of Materials**). Obtain probes for the genes of interest and buffers and solutions from the supplier. All incubation steps are performed at RT, if not mentioned otherwise. Use sterile PBS. If interested in staining several SG in one well, use at least 150 µL of buffers and solutions.

3.1. Perform dissection of the SG as described in steps 1.1–1.13.

3.2. Fixate SG for 1 h in 200 µL of 4% MeOH-free PFA/PBS in one well of a 96-well plate placed on an orbital shaker.

3.3. Wash SG three times for 30 min each in 0.1% Tween-20/PBS on an orbital shaker.

3.4. Dehydrate SG in MeOH/PBS series by subsequent incubation in 50% MeOH/PBS, 70% MeOH/PBS, and 100% MeOH for 10 min each on an orbital shaker.

3.5. Store SG at -20 °C in 100% MeOH overnight.

3.6. The next day, pre-warm the incubator to 40 °C. Check the temperature with a thermometer.

3.7. Rehydrate SG in reverse MeOH/PBS series (100% MeOH, 70% MeOH/PBS, 50% MeOH/PBS) for 10 min each.

3.8. Wash SG three times for 5 min each in PBS.

3.9. In the meantime, start pre-warming the probes by incubation at 40 °C for 10 min, followed by cooling for 10 min.

3.10. Incubate SG in 200 µL of Protease III for 15 min.

3.11. Optional: Perform Sudan black treatment to quench autofluorescence according to sections 2.3, 2.7, and 2.8 of this protocol if subsequent immunofluorescence staining is planned.

3.12. Wash SG in 200 µL of 0.1% Tween-20/PBS 3x for 5 min each on an orbital shaker.

3.13. Optional: If co-staining with several probes is desired, dilute Channel-2 (50x) and Channel-3 probe (50x) in Channel-1 probe (1x).

3.14. Cover SG with 100 µL of probe for the gene of interest and incubate overnight at 40 °C with slight agitation. Place the 96-well plate in a wet chamber at 40 °C for all incubation steps.

NOTE: Include one SG as negative control, using a probe against a bacterial gene (e.g., dihydro-

dipicolinate reductase, *Dapb*) to check for non-specific binding of amplification reagents in later steps.

3.15. Wash SG in supplied washing buffer 3x for 15 min each on an orbital shaker.

3.16. Pre-warm Amp1-3, HRP-C1, and HRP-Blocker to RT. If co-staining with Channel-2 and/or Channel-2 probe is desired, pre-warm HRP-C2 and HRP-C3.

3.17. Re-fix SG for 10 min at RT in 4% PFA/PBS on an orbital shaker.

3.18. Wash SG in 200 µL of supplied washing buffer 3x for 5 min each on an orbital shaker at RT.

3.19. For amplification, incubate SG with 100 µL of Amp1 for 35 min at 40 °C on an orbital shaker.

3.20. Carefully remove any liquid and wash SG in 200 µL of supplied washing buffer 3x for 5 min each at RT on an orbital shaker.

3.21. Incubate SG with 100 µL of Amp2 for 35 min at 40 °C on an orbital shaker.

3.22. Repeat step 3.18.

3.23. Incubate SG with 100 µL of Amp3 for 20 min at 40 °C on an orbital shaker.

3.24. Repeat step 3.18.

3.25. Incubate SG with 100 µL of supplied Multiplex FL v2 HRP-C1 for 20 min at 40 °C on an orbital shaker.

3.26. Repeat step 3.18.

3.27. Prepare Opal-conjugated secondary antibody 1:1,000 in 200 µL of supplied TSA-buffer and incubate SG for 35 min at 40 °C on an orbital shaker. Protect from light during incubation and from this step on.

3.28. Repeat step 3.18.

3.29. Incubate SG in 100 µL of supplied Multiplex FL v2 HRP-blocker for 15 min at 40 °C on an orbital shaker.

3.30. Repeat step 3.18.

3.31. Optional: For co-staining with Channel-2 probe, repeat steps 3.25–3.30 with supplied Multiplex FL v2 HRP-C2.

3.32. Optional: For co-staining with Channel-3 probe, repeat steps 3.25–3.30 with supplied Multiplex FL v2 HRP-C3.

3.33. In case of subsequent immunofluorescent staining, perform steps 2.14–2.25 of this protocol.

3.34. Incubate in 1% BSA/PBS for 30 min on an orbital shaker.

3.35. Incubate SG for 30 min in 1 µg/mL of bisbenzimide H33342 trihydrochloride (Hoechst staining) in 1% BSA/PBS if nuclear staining is desired and/or add Alexa-coupled wheat germ agglutinin (WGA, 1:500) on an orbital shaker.

3.36. Repeat step 3.18.

3.37. Embed as described in steps 2.19–2.22.

## 4. Imaging and analyses of murine stellate ganglia

4.1. Perform confocal microscopy of embedded SG in the local imaging facility.

4.2. If cell size measurements are required, image SG stained for tyrosine hydroxylase (see **Table of Materials**) at 200x magnification and take 4–6 random images from every SG.

4.3. Analyze images using ImageJ[33] software to estimate cell size (e.g., with a pen table, see **Table of Materials**). Use **Free Hand Selection**, circle each cell and click on **Analyze | Measure** to obtain cell area. Be careful to include only intact, fully visible cells that are located well within the SG.

4.4. Using this method, perform measurement of approximately 100 cells per SG.

4.5. Have a blinded investigator perform steps 4.2–4.3 if you want to compare SG from different mice. Use a frequency distribution in statistical software to visualize size differences between groups[34].

## 5. Molecular analyses of murine stellate ganglia

NOTE: Include controls depending on your experimental design. This could be SG with different genotypes and disease background and/or other autonomic ganglia, such as the sympathetic superior cervical ganglion (located in the neck area, see detailed description in Ziegler et al.[35]) or parasympathetic ganglia (such as intracardiac ganglia, see Jungen et al.[4]).

5.1. Prepare a 2 mL tube with 500 µL of phenol/guanidine thiocyanate solution (e.g., Qiazol) per animal and have liquid nitrogen ready for shock-frosting or consider commercial solutions for protection of RNA (optional, see **Table of Materials**)[36]. Work quickly for RNA isolation.

5.2. Perform dissection of the SG as described in steps 1.1–1.13.

5.3. Immediately immerse both SG directly in one tube with phenol/guanidine thiocyanate solution and shock-frost tube in liquid nitrogen.

5.4. Store at -80 °C until further processing.

5.5. For tissue lysis, let tubes with SG thaw until phenol/guanidine thiocyanate solution is liquified and add two 7 mm stainless steel beads. Cool down the metal parts of tissue homogenizer (ball or mixer mill, e.g., Tissue Lyser II) on dry ice and centrifuge to 4 °C.

5.6. Centrifuge tubes at 500 x *g* for 1 min at 4 °C so that SG are at the bottom of the tube.

5.7. Put tubes into the metal parts of the Tissue Lyser and lyse for 1 min at 20 Hz.

5.8. Repeat steps 5.6 and 5.7 up to 5 times until no intact tissue is detectable.

5.9. Transfer the liquid into a fresh 1.5 mL tube.

5.10. Perform RNA isolation with a column-based RNA isolation kit (e.g., miRNeasy mini kit) according to the manufacturer's instructions.

5.11. Elute RNA in 20 µL of RNase-free water and measure concentration using a spectrophotometer.

NOTE: To exclude contamination of the purified RNA with genomic DNA, we propose performing a polymerase chain reaction with genomic primers and 1 µL of RNA as template, instead minus reverse transcriptase control. This will save a significant amount of RNA. If RNA is contaminated, use exon-intron boundary primers or intron flanking primers for subsequent quantitative real-time polymerase chain reaction.

5.12. Use 250 ng SG RNA to perform cDNA synthesis and use established protocols. Here a high-capacity cDNA reverse transcription kit was used according to the manufacturer's instructions.

5.13. Dilute to a final concentration of 2.5 ng/µL of cDNA and perform quantitative real-time polymerase chain reaction with the appropriate probes according to the established protocols. Here TaqMan Assay (**see Table of Materials**) was performed using 10 ng cDNA per reaction.

NOTE: Perform no-template control for every gene to exclude false positive results.

5.14. Normalize gene expression of your gene of interest on a house keeping gene (e.g., *Cdkn1b*) to compare relative gene expression between different groups of SG.

**REPRESENTATIVE RESULTS:**

**Figure 1** visualizes how to identify and dissect the SG. **Figure 1A** shows a schematic drawing of the location, while **Figure 1B** presents the view of the thorax after removal of the heart-lung-package. The left and right longus colli muscles medial from the SG and the rib cage are important landmarks for orientation. Dissection is performed along the dotted lines between muscles and the first rib. The SG and the sympathetic chain become visible as white structures (**Figure 1C**). **Figure 1D** shows a magnification of the region between the left longus colli muscle and the first rib, where the left SG is located. Morphology of the SG differs between individuals. It often consists of a fusion of the inferior cervical and the first to the third thoracic ganglia[24]. Some variety that the experimenter can expect in murine SG is depicted in **Figure 1E**,**F**, where left and right SG of five male C57Bl6 wild type mice are photographed.

The gross anatomic overview, cellular and subcellular analyses of cells in the SG innervating the heart can be performed by whole mount techniques on protein and RNA level. An overview of a SG is presented in **Figure 2**. Myocardial sympathetic fibers originate from cell bodies in the SG. These are visualized by staining with an antibody against tyrosine hydroxylase (TH). TH-expressing neuronal somata are surrounded by nerve fibers staining positive for choline acetyltransferase (ChAT). These are most likely presynaptic fibers[37,38]. An exemplary magnification from TH and ChAT co-labeling is presented in **Figure 2A**. Glial cells surrounding neuronal cell bodies can be visualized by staining for S100B. This is depicted in **Figure 2B** in combination with the neural marker PGP9.5. **Figure 2C–F** show exemplary analyses to study the SG on a subcellular level, using whole mount in situ hybridization and immunofluorescent co-staining. The protein TH (**Figure 2C**, red) and mRNA molecules of *Tubb3* (**Figure 2D**, white) are expressed in large neuronal cell bodies, while mRNA of *S100b* (**Figure 2E**, green) is also detectable in surrounding glia cells. In the merge (**Figure 2F**), it is visible that some neurons are negative for TH but express *Tubb3*, while *S100b* mRNAs can also be detected in surrounding cells, as depicted in the magnification in **Figure 2G**.

**Figure 3** presents potential quantitative analyses and pitfalls for studying the murine SG. Images from TH-stained SG (**Figure 3A)** can be used for cell size measurements as was performed exemplary for a mouse model of diabetes. Neuronal somata from control (db/het) SG were 388.8 ± 123.8 $\mu m^2$ vs. in diabetic SG (db/db) 407.33 ± 139.6 $\mu m^2$ (**Figure 3B**, n = 2 SG, 100 cells per SG per genotype, $P$ = 0.348, data were compared using Mann-Whitney test). **Figure 3C** shows the expression of genes from different cell types of the SG (n = 6–7). Pooling of both SG from one animal allows gene expression measurements of approximately 24 assays (12 genes in duplicates). We typically normalize samples for *Cdkn1b* (detected at Ct values of 25.4 ± 0.97) as well as the neuronal marker *Neun/Rbfox3* (32.5 ± 0.7) if it is necessary to account for other cell types and neuronal purity of the dissection. Genes that we found useful for characterizing molecular processes in the SG include the sympathetic gene *Th* (22.4 ± 1.6), *Chat*, which could indicate cholinergic transdifferentiation (expressed at Ct values of 30.8 ± 1.3) and *Gap43*, a marker for neuronal

sprouting (detectable at Ct values of 22.4 ± 1.4). Genes expressed in non-neuronal cell type include *S100b* (for glial cells, 27.3 ± 1.2), *Ki-67* (for proliferating cells, 33.0 ± 1.6) and *Cd45* (for immune cells, 30.2 ± 1.1).

The SG is surrounded by a capsule of connective tissue[26], visualized via hematoxylin and eosin staining in **Figure 3D,E**. Occasionally, we observed inconsistencies in antibody-based staining as demonstrated in **Figure 3F**, most likely due to incomplete removal of the capsule. While ChAT and TH staining are only detectable in some parts of the SG, nuclei counterstained with DAPI are detectable throughout. The dotted line in the merged image separates successful staining (right of the line) from unsuccessful staining (left of the line).

Data are presented as mean ± standard deviation. Statistical significance was defined as a P value of <0.05; statistical analysis was performed using commercial software.

**FIGURE AND TABLE LEGENDS:**

**Figure 1: Location, dissection, and morphology of the murine stellate ganglia.** (**A**) Schematic drawing of the location of the stellate ganglia (SG). (**B**) View into the thorax after removal of the heart-lung package. It is important to note that the SG are not immediately visible most of the time. The longus colli muscles are located lateral from the spine. The SG are located lateral from the muscles at the junction with the first rib. Carefully dissect lateral to the muscles (area marked by dotted line) to uncover the ganglia. After dissection, ganglia (left and right, LSG and RSG, respectively) and the sympathetic chain can be made out as white, long structures. (**C**) An exemplary dissection showing the ganglia and anatomical landmarks. (**D**) Magnification of the LSG. (**E**) LSG and (**F**) RSG from wild type, male C57Bl6 mice (16 weeks) were dissected and photographed to show the variations in morphology and size. Scale bar represents 1,000 µm.

**Figure 2: Visualization of different cell types in murine stellate ganglia via whole mount immunohistochemistry and in situ hybridization.** (**A**) Gross overview of a murine stellate ganglion (SG) stained for the sympathetic marker tyrosine hydroxylase (TH) and choline acetyltransferase (ChAT). The magnification shows TH-positive cell bodies and the presence of ChAT-positive, most likely presynaptic, nerve fibers surrounding neuronal somata. (**B**) Glial cells ensheathing neuronal cell bodies can be visualized by staining for S100B, here in combination with the neuronal marker PGP9.5. (**C–F**) Microscopic images from one SG stained whole mount via a combination of immunohistochemistry for TH (red) and in situ hybridization for *Tubb3* (D, white) and *S100b* (E, green). Nuclei are counterstained with DAPI (blue). (**F**) The merge shows that not all neuronal (*Tubb3*-positive) cells are TH positive. *S100b* mRNAs can be detected within neuronal somata, but also surrounding cells, as marked by an arrow in the magnification in (**G**).

**Figure 3**: **Potential quantitative analyses and pitfalls**. (**A**) Images from Tyrosine-hydroxylase (TH)-stained SG can be used for cell size measurements using ImageJ. (**B**) This was performed in a mouse model of diabetes (100 cells per SG, n = 2 SG per genotype, data was compared using Mann-Whitney test). (**C**) Exemplary genes expressed in the SG that might be useful for characterizing molecular processes. *Cdkn1b* as well as the neuronal marker *Neun/Rbfox3* (to account for

the presence of other cell types) can be used for normalization. Tyrosine hydroxylase (*Th*) serves as a sympathetic marker, choline acetyltransferase (*Chat*) for cholinergic transdifferentiation, *Gap43* for neuronal sprouting. Genes expressed in non-neuronal cell types include *S100b* (glial cells), *Ki-67* (proliferating cells) and *Cd45* (immune cells). (**D**) Hematoxylin and eosin staining of a formalin-fixed SG visualizes connective tissue and cells on top of the SG. (**E**) Magnification from the boxed area. (**F**) On some occasions, we observed failure in antibody-based staining, most likely due to incomplete removal of the capsule. While ChAT (red) and TH (green) staining are only detectable in some parts of the SG, nuclei counterstained with DAPI (dark blue) are detectable throughout. The dotted line in the merged image separates successful staining (right of the line) from unsuccessful staining (left of the line).

**DISCUSSION:**

The understanding of cellular and molecular processes in neurons and glial cells of the sympathetic nervous system that precede the onset of VA is of high interest, as sudden cardiac arrest remains the most common cause of death worldwide[5]. Therefore, in the current manuscript, we provide a basic repertoire of methods to identify the murine SG—a key element within this this network—and perform subsequent analyses on RNA, protein, and cellular level.

One challenge of the murine SG is its size and the limited number of cells[39]. Due to this, different animal models, such as rats[40], dogs[22], and pigs[41] are used for studies on the SG. Still, there is a variety of well-established disease models for cardiac phenotypes available in mice and some of these have already been characterized in different aspects of cardiac innervation and arrhythmia, such as models for diabetes[23], myocardial infarction[42], or myocarditis[43]. Therefore, further studies of the murine SG are warranted to further characterize autonomic dysfunction in the light of VA. These can be completed by other approaches to study innervation of the murine heart as functional experiments[4,23,44] including in-vivo stimulation of the SG[23].

Due to its small size and its location within the thoracic cavity[24], manipulation of the murine SG in vivo is challenging, although it has been performed successfully[23]. For this reason, some studies therefore focus on the superior cervical ganglia, which are located more accessibly in the neck, upstream of the SG in the sympathetic chain behind the carotid bifurcation into internal and external carotid arteries[24,35]. Cardiac denervation via removal of the superior cervical ganglia has been shown to attenuate myocardial inflammation, hypertrophy, and cardiac dysfunction after myocardial infarction[35]. However, it is important to note that the superior cervical ganglia innervate different regions of the heart, most prominently the anterior side[45]. In addition, a recent in-depth literature review came to the conclusion that the role of cervical ganglia on sympathetic innervation of the heart remains unclear in humans[46]. This highlights the importance of characterizing the SG for studies of cardiac sympathetic innervation.

It is important to note that the heart is not the only target of the SG. Among others, lungs[47] and sweat glands in the forepaw[48] are also innervated from fibers originating in the SG, the latter are an exception to sympathetic physiology as they express choline acetyltransferase[37]. Temporary blockade of the SG is studied with regard to inflammatory processes in acute lung injury[49] or for treatment of hot flushes and sleep dysfunction[50]; therefore, the protocols at hand might offer a

repertoire for mechanistic questions in these fields. When focusing on cardiac disease models, it should be kept in mind for interpretation of results that cardiac neurons cannot be differentiated by morphology or electrophysiological properties from non-cardiac neurons[51]. This can be achieved by retrograde tracing, thereby the location of neurons projecting to the heart was shown to be located in the cranio-medial parts of the SG[52].

Additionally, it is important to note that besides different types of neurons, sympathetic ganglia are made up of ensheathing glia, so-called satellite glial cells or satellite cells marked by expression of the glial marker S100B[53]. While little is known about the role of these cells in cardiovascular pathologies, glial activation and expression of the glial fibrillary acidic protein (GFAP) has been described in SG from patients with arrhythmias[18].

Some pitfalls should be kept in mind with the presented methods: we observed inconsistencies in antibody-based staining at some occasions and hypothesized that incomplete removal of the connective tissue capsule ensheathing the SG might be at fault, as they have been described to vary in permeability among different types of ganglia[26]. Mechanical removal of the capsule using fine forceps has been described in the superior cervical ganglion of rats up to postnatal day 10[28] and desheathing is mentioned in literature for adult rat SG[54,55] and mice[56]. Removal of the SG capsule might vary between age[28] and – due to size differences – species. In our experience, fresh dissection, removal of as much connective tissue as possible using fine forceps and thorough permeabilization as described in the protocol at hand, are important factors for successful staining. Regarding quantitative real-time PCR, quick work and efficient lysis are essential. Pooling both SGs from one animal reliably allowed for the analysis of up to 12 different genes (when performing duplicates).

Even though function and gross anatomy of SG has been studied for decades now and every single cardiomyocyte is innervated by sympathetic fibers[46], many open questions remain. For example, it remains unclear, why sympathetic neurons of the SG transdifferentiate transiently to a cholinergic phenotype in ischemic[21] and non-ischemic heart failure, in animal models as well as in patients[20]. Recently, our group described a role of S100B-positive glial cells, which are also present in the murine SG, on nerve sprouting in the cardiac nervous system[29]. Whether these cells are relevant for sympathetic nerve sprouting after injury associated with VA[11,12], needs to be elucidated in future studies. Importantly, innovative approaches, such as optogenetics[52] and transcriptome analyses[36] can complement established methods such as neuronal tracing in order to deepen the understanding of the sympathetic nervous system and its role on cardiac electrophysiology.

In conclusion, this repertoire allows the inexperienced investigator to perform a basic characterization of the SG in murine models of cardiac pathologies. We hope that this will stimulate the usage, combination, and creation of novel methods. This might help to increase the understanding of the underlying cellular and molecular processes in sympathetic neurons that might be responsible for the onset and maintenance of VA.

**ACKNOWLEDGMENTS:**

The authors would like to thank Hartwig Wieboldt for his excellent technical assistance, and the UKE Microscopy Imaging Facility (Umif) of the University Medical Center Hamburg-Eppendorf for providing microscopes and support. This research was funded by the DZHK (German Centre for Cardiovascular Research) [FKZ 81Z4710141].

**DISCLOSURES:**

The authors have nothing to disclose.

**REFERENCES:**

1. Goldberger, J. J., Arora, R., Buckley, U., Shivkumar, K. Autonomic nervous system dysfunction: JACC focus seminar. *Journal of the American College of Cardiology*. **73** (10), 1189–1206 (2019).
2. Jänig, W. Neurocardiology: a neurobiologist's perspective. *The Journal of Physiology*. **594** (14), 3955–3962 (2016).
3. Meng, L., Shivkumar, K., Ajijola, O. Autonomic Regulation and Ventricular Arrhythmias. *Current Treatment Options in Cardiovascular Medicine*. **20** (5) (2018).
4. Jungen, C. et al. Disruption of cardiac cholinergic neurons enhances susceptibility to ventricular arrhythmias. *Nature Communications*. **8**, 14155 (2017).
5. Al-Khatib, S.M. *et al.* 2017 AHA/ACC/HRS Guideline for management of patients with ventricular arrhythmias and the prevention of sudden cardiac death. *Circulation*. **138** (13), e272–e391 (2018).
6. Yusuf, S., Wittes, J., Friedman, L. Overview of results of randomized clinical trials in heart disease: I. treatments following myocardial infarction. *JAMA: The Journal of the American Medical Association*. **260** (14), 2088–2093 (1988).
7. Sapp, J. L. et al. Ventricular tachycardia ablation versus escalation of antiarrhythmic drugs. *New England Journal of Medicine*. **375** (2), 111–121 (2016).
8. Yasunaga, K., Nosaka, S. Cardiac sympathetic nerves in rats: Anatomical and functional features. *The Japanese Journal of Physiology*. **29** (6) (1979).
9. Pardini, B. J., Lund, D. D., Schmid, P. G. Organization of the sympathetic postganglionic innervation of the rat heart. *Journal of the Autonomic Nervous System*. **28** (3), 193–201 (1989).
10. Meyer, C., Scherschel, K. Ventricular tachycardia in ischemic heart disease: The sympathetic heart and its scars. *American Journal of Physiology - Heart and Circulatory Physiology*. **312** (3), H549–H551 (2017).
11. Cao, J. M. et al. Relationship between regional cardiac hyperinnervation and ventricular arrhythmia. *Circulation*. **101** (16), 1960–1969 (2000).
12. Ren, C. et al. Nerve sprouting suppresses myocardial Ito and IK1 channels and increases severity to ventricular fibrillation in rat. *Autonomic Neuroscience: Basic and Clinical*. **144** (1–2), 22–29 (2008).
13. Zipes, D.P. et al. Treatment of ventricular arrhythmia by permanent atrial pacemaker and cardiac sympathectomy. *Annals of Internal Medicine*. **68** (3), 591–597 (1968).
14. Kusumoto, F. M. et al. Systematic review for the 2017 AHA/ACC/HRS guideline for management of patients with ventricular arrhythmias and the prevention of sudden cardiac death. *Circulation*. **138** (13) (2018).
15. Cronin, E. M. et al. 2019 HRS/EHRA/APHRS/LAHRS Expert Consensus Statement on

Catheter Ablation of Ventricular Arrhythmias: Executive Summary. *Heart Rhythm*. (2019).
16. Vaseghi, M. et al. Cardiac sympathetic denervation in patients with refractory ventricular arrhythmias or electrical storm: Intermediate and long-term follow-up. *Heart Rhythm*. **11** (3), 360–366 (2014).
17. Vaseghi, M. et al. Cardiac sympathetic denervation for refractory ventricular arrhythmias. *Journal of the American College of Cardiology*. **69** (25), 3070–3080 (2017).
18. Ajijola, O. A. et al. Inflammation, oxidative stress, and glial cell activation characterize stellate ganglia from humans with electrical storm. *JCI insight*. **2** (18), 1–11 (2017).
19. Rizzo, S. et al. T-cell-mediated inflammatory activity in the stellate ganglia of patients with ion-channel disease and severe ventricular arrhythmias. *Circulation: Arrhythmia and Electrophysiology*. **7** (2), 224–229 (2014).
20. Kanazawa, H. et al. Heart failure causes cholinergic transdifferentiation of cardiac sympathetic nerves via gp130-signaling cytokines in rodents. *Journal of Clinical Investigation*. **120** (2), 408–421 (2010).
21. Olivas, A. et al. Myocardial infarction causes transient cholinergic transdifferentiation of cardiac sympathetic nerves via gp130. *Journal of Neuroscience*. **36** (2), 479–488 (2016).
22. Yu, L. et al. Optogenetic Modulation of Cardiac Sympathetic Nerve Activity to Prevent Ventricular Arrhythmias. *Journal of the American College of Cardiology*. **70** (22), 2778–2790 (2017).
23. Jungen, C. et al. Increased arrhythmia susceptibility in type 2 diabetic mice related to dysregulation of ventricular sympathetic innervation. *American Journal of Physiology - Heart and Circulatory Physiology*. **317** (6), H1328–H1341 (2019).
24. Hedger, J. H., Webber, R. H. Anatomical study of the cervical sympathetic trunk and ganglia in the albino rat (Mus norvegicus albinus). *Acta Anatomica*. **96** (2), 206–217 (1976).
25. Furlan, A. et al. Visceral motor neuron diversity delineates a cellular basis for nipple- and pilo-erection muscle control. *Nature Neuroscience*. **19** (10), 1331–1340 (2016).
26. Al Khafaji, F. A. H., Anderson, P. N., Mitchell, J., Mayor, D. The permeability of the capsule of autonomic ganglia to horseradish peroxidase. *Journal of Anatomy*. **137** (4), 675–682 (1983).
27. Armour, J. A., Murphy, D. A., Yuan, B. X., Macdonald, S., Hopkins, D. A. Gross and microscopic anatomy of the human intrinsic cardiac nervous system. *Anatomical Record*. **247** (2), 289–298 (1997).
28. Fedoroff, S., Richardson, A., Johnson, M. I. Primary Cultures of Sympathetic Ganglia. *Protocols for Neural Cell Culture*. (11051), 71–94 (2003).
29. Scherschel, K. et al. Cardiac glial cells release neurotrophic S100B upon catheter-based treatment of atrial fibrillation. *Science Translational Medicine*. **11** (493), 1–12 (2019).
30. Sun, Y. et al. Sudan black B reduces autofluorescence in murine renal tissue. *Archives of Pathology and Laboratory Medicine*. **135** (10), 1335–1342 (2011).
31. Alanentalo, T. et al. Tomographic molecular imaging and 3D quantification within adult mouse organs. *Nature Methods*. **4** (1), 31–33 (2007).
32. Kersigo, J. et al. A RNAscope whole mount approach that can be combined with immunofluorescence to quantify differential distribution of mRNA. *Cell and Tissue Research*. **374** (2), 251–262 (2018).
33. Schindelin, J. et al. Fiji: An open-source platform for biological-image analysis. *Nature Methods*. **9** (7), 676–682 (2012).

34. Bassil, G. et al. Pulmonary vein ganglia are remodeled in the diabetic heart. *Journal of the American Heart Association*. **7** (23) (2018).
35. Ziegler, K. A. et al. Local sympathetic denervation attenuates myocardial inflammation and improves cardiac function after myocardial infarction in mice. *Cardiovascular Research*. **114** (2), 291–299 (2018).
36. Bayles, R.G. et al. Transcriptomic and neurochemical analysis of the stellate ganglia in mice highlights sex differences. *Scientific Reports*. **8** (1), 8963 (2018).
37. Morales, M.A. et al. Localization of choline acetyltransferase in rat peripheral sympathetic neurons and its coexistence with nitric oxide synthase and neuropeptides. *Proceedings of the National Academy of Sciences of the United States of America*. **92** (25), 11819–11823 (1995).
38. Jimnez, B., Mora-Valladares, E., Zetina, M. E., Morales, M. A. Occurrence, co-occurrence and topographic distribution of choline acetyl transferase, met-enkephalin and neurotensin in the stellate ganglion of the cat. *Synapse*. **43** (3), 163–174 (2002).
39. Ruit, K. G., Osborne, P. A., Schmidt, R. E., Johnson, E. M., Snider, W. D. Nerve growth factor regulates sympathetic ganglion cell morphology and survival in the adult mouse. *Journal of Neuroscience*. **10** (7), 2412–2419 (1990).
40. Guo, J. et al. Involvement of P2Y 12 receptor of stellate ganglion in diabetic cardiovascular autonomic neuropathy. *Purinergic Signalling*. **14** (4), 345–357 (2018).
41. Ajijola, O. A. et al. Remodeling of stellate ganglion neurons after spatially targeted myocardial infarction: Neuropeptide and morphologic changes. *Heart Rhythm*. **12** (5), 1027–1035 (2015).
42. Hinrichs, S. et al. Precursor proadrenomedullin influences cardiomyocyte survival and local inflammation related to myocardial infarction. *Proceedings of the National Academy of Sciences of the United States of America*. **115** (37), E8727–E8736 (2018).
43. Westermann, D. et al. Reduced degradation of the chemokine MCP-3 by matrix metalloproteinase-2 exacerbates myocardial inflammation in experimental viral cardiomyopathy. *Circulation*. **124** (19), 2082–2093 (2011).
44. Johnsen, D., Olivas, A., Lang, B., Silver, J., Habecker, B. Disrupting protein tyrosine phosphatase σ does not prevent sympathetic axonal dieback following myocardial infarction. *Experimental Neurology*. **276**, 1–4 (2016).
45. Manousiouthakis, E., Mendez, M., Garner, M. C., Exertier, P., Makita, T. Venous endothelin guides sympathetic innervation of the developing mouse heart. *Nature Communications*. **5** (May), 3918 (2014).
46. Wink, J. et al. Human adult cardiac autonomic innervation: Controversies in anatomical knowledge and relevance for cardiac neuromodulation. *Autonomic Neuroscience*. **227** (April), 102674 (2020).
47. Kummer, W., Fischer, A., Kurkowski, R., Heym, C. The sensory and sympathetic innervation of guinea-pig lung and trachea as studied by retrograde neuronal tracing and double-labelling immunohistochemistry. *Neuroscience*. **49** (3), 715–737 (1992).
48. Schäfer, M. K. H., Schütz, B., Weihe, E., Eiden, L. E. Target-independent cholinergic differentiation in the rat sympathetic nervous system. *Proceedings of the National Academy of Sciences of the United States of America*. **94** (8), 4149–4154 (1997).
49. Chen, Y. et al. Effect of a Stellate Ganglion block on acute lung injury in septic rats. *Inflammation*. **41** (5), 1601–1609 (2018).

50. Lipov, E. G. et al. Effects of stellate-ganglion block on hot flushes and night awakenings in survivors of breast cancer: a pilot study. *The Lancet Oncology*. **9** (6), 523–532 (2008).
51. Mo, N., Wallis, D. I., Watson, A. Properties of putative cardiac and non-cardiac neurones in the rat stellate ganglion. *Journal of the Autonomic Nervous System*. **47** (1–2), 7–22 (1994).
52. Rajendran, P. S. et al. Identification of peripheral neural circuits that regulate heart rate using optogenetic and viral vector strategies. *Nature Communications*. **10** (1), 1–13 (2019).
53. Hanani, M. Satellite glial cells in sympathetic and parasympathetic ganglia: In search of function. *Brain Research Reviews*. **64** (2), 304–327 (2010).
54. Larsen, H. E., Lefkimmiatis, K., Paterson, D. J. Sympathetic neurons are a powerful driver of myocyte function in cardiovascular disease. *Scientific Reports*. **6**, 1–11 (2016).
55. Hasan, W. et al. Sympathetic hyperinnervation and inflammatory cell NGF synthesis following myocardial infarction in rats. *Brain Research*. **1124** (1), 142–154 (2006).
56. Lorentz, C. U. et al. Heterogeneous ventricular sympathetic innervation, altered β-adrenergic receptor expression, and rhythm instability in mice lacking the p75 neurotrophin receptor. *American Journal of Physiology - Heart and Circulatory Physiology*. **298** (6), 1652–1660 (2010).

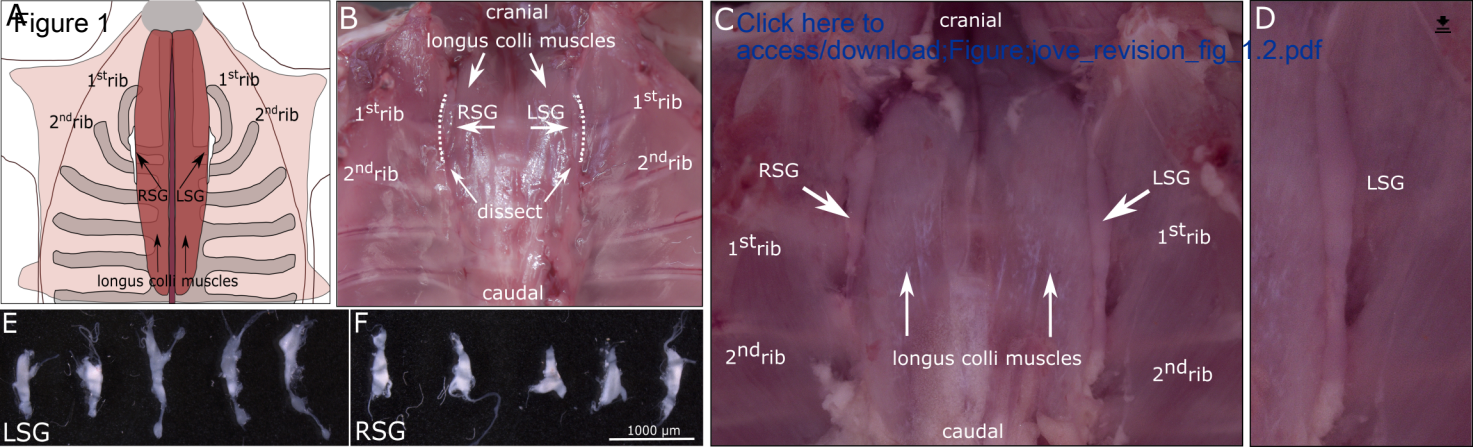
Figure 1
A
1st rib
1st rib
2nd rib
2nd rib
RSG
LSG
longus colli muscles
B
cranial
longus colli muscles
1st rib
RSG
LSG
1st rib
2nd rib
2nd rib
dissect
caudal
C
Click here to access/download;Figure;jove_revision_fig_1.2.pdf
cranial
RSG
LSG
1st rib
1st rib
2nd rib
longus colli muscles
2nd rib
caudal
D
LSG
E
LSG
F
RSG
1000 µm

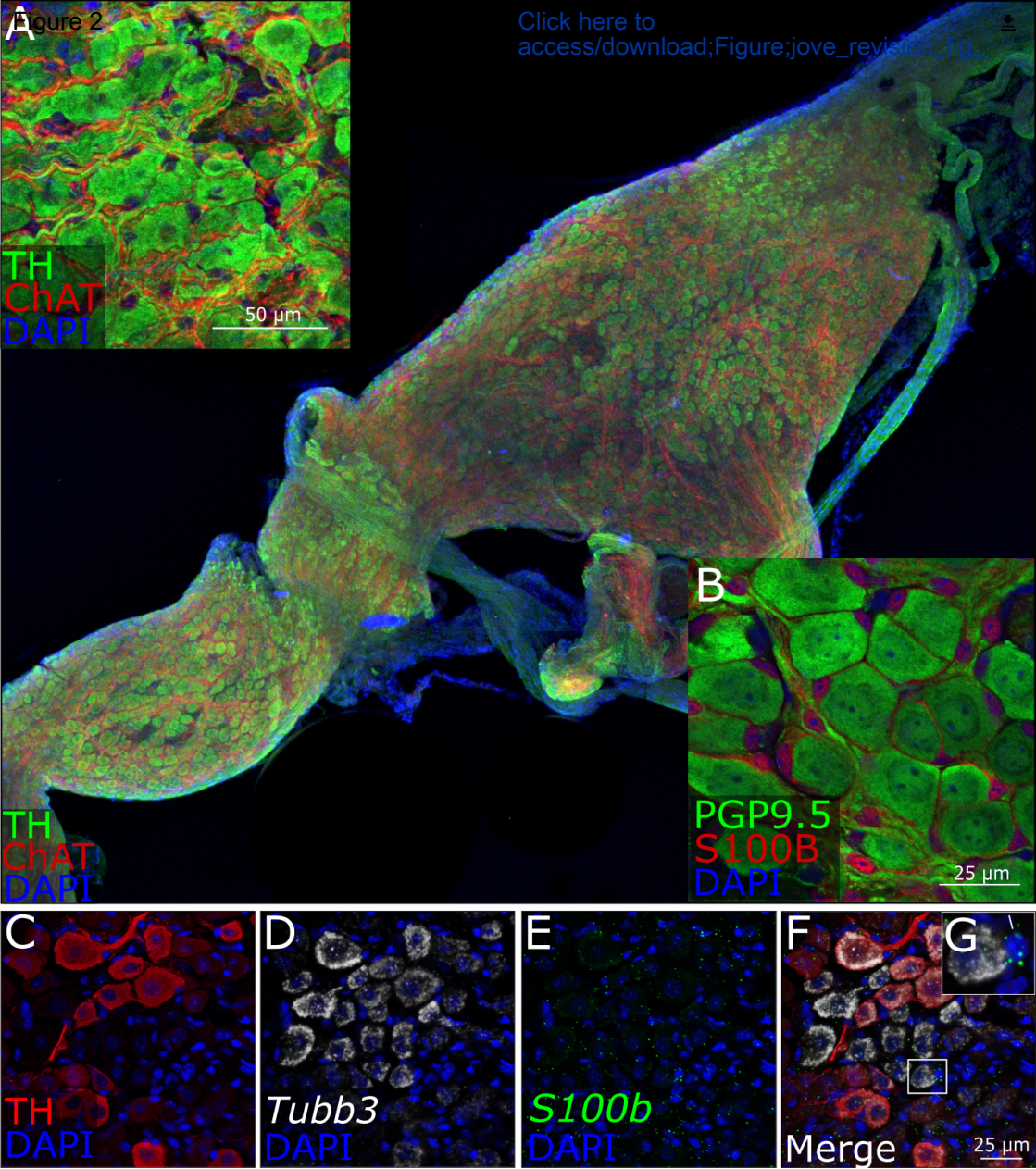

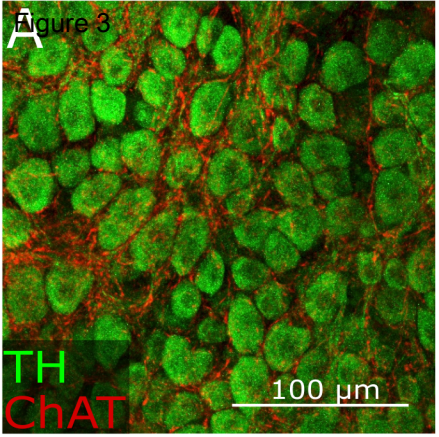


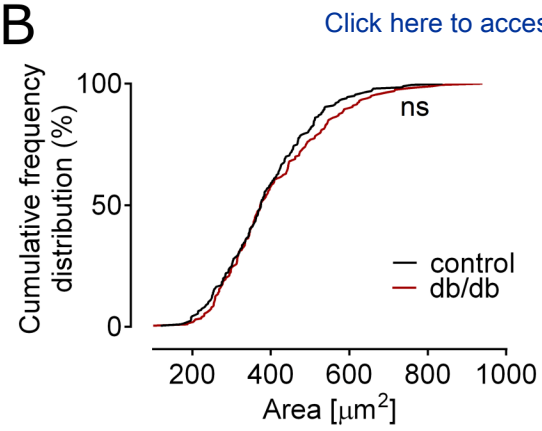


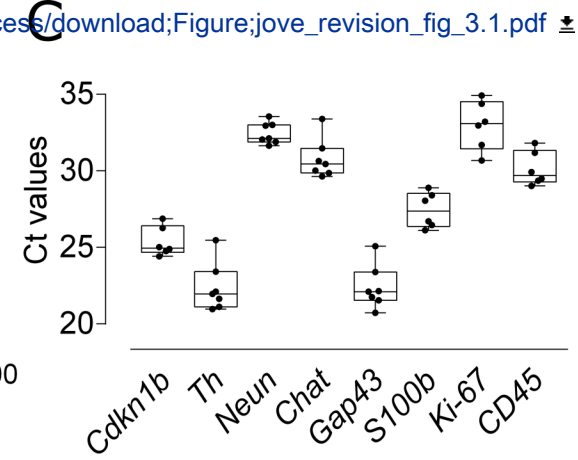


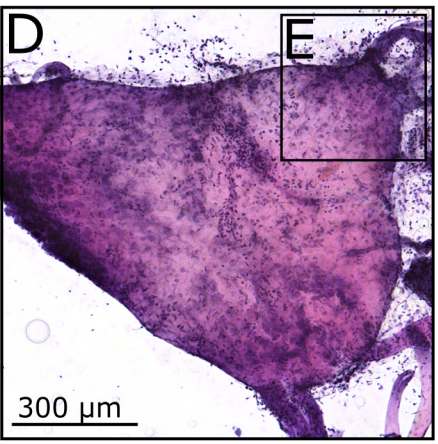


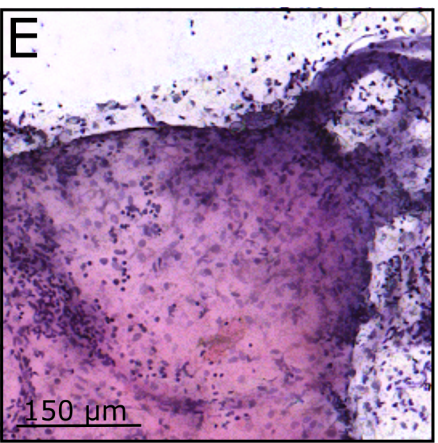


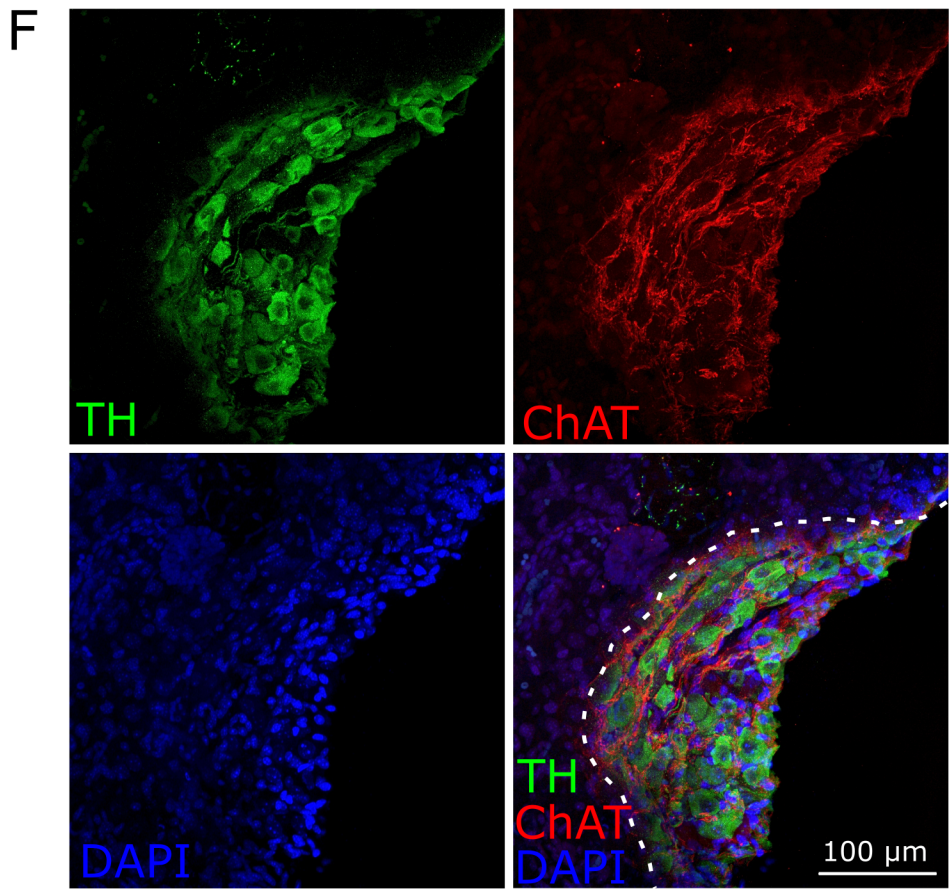

**Name of Material/ Equipment**

96-well plate
Adhesion Slides SuperFrost plus 25 x 75 x 1 mm
Albumin bovine Fraction V receptor grade lyophil.
bisBenzimide H33342 trihydrochloride (Hoechst)
Chicken anti neurofilament
Dimethyl sulfoxide (DMSO)
Donkey anti chicken IgY Alexa 647
Donkey anti goat IgG Alexa 568
Donkey anti rabbit IgG Alexa 488
Drying block 37-100 mm
Eosin Y
Ethanol 99 % denatured with MEK, IPA and Bitrex (min. 99,8 %)
Eukitt mounting medium
Fluoromount-G
Fluoromount-G + DAPI
Goat anti choline acetyltransferase
$H_2O_2$ 30% (w/w)
Heparin Sodium 25.000 UI / 5ml
High-capacity cDNA reverse transctiption kit
Isoflurane (Forene)
Mayer's hemalum solution
Methanol
Microscope cover glasses 20x20 mm or smaller
miRNeasy Mini Kit
NanoDrop 2000c
Opal 570 Reagent Pack
Paraformaldehyde, 16% w/v aq. soln., methanol free
Pasteur pipettes, LDPE, unsterile, 3 ml, 154 mm
Phosphate-buffered saline tablets
Pinzette Dumont SS Forceps
QIAzol Lysis Reagent
Rabbit anti tyrosine hydroxylase
RNAlater
RNAscope Multiplex Fluorescent Reagent Kit v2
RNAscope Probe-Mm-S100b-C2
RNAscope Probe-Mm-Tubb3
Stainless steel beads 7 mm
Sudan black B
TaqMan Gene Expression Assay Cdkn1b (Mm00438168_m1)
TaqMan Gene Expression Assay Choline acetyltransferase (Mm01221880_m1)
TaqMan Gene Expression Assay MKi67 (Mm01278617_m1)
TaqMan Gene Expression Assay PTPCR (Mm01293577_m1)
TaqMan Gene Expression Assay S100b (Mm00485897_m1)
TaqMan Gene Expression Assay Tyrosin Hydroxylase (Mm00447557_m1)
TaqMan mastermix
Tissue Lyser II
Triton X-100 10% solution
Tween-20
Wacom bamboo pen
Whatman prepleated qualitative filter paper, Grade 595 1/2

Wheat Germ Agglutinin, Alexa Fluor 633 Conjugate

| Company | Catalog Number |
|---|---|
| TPP | 92097 |
| R. Langenbrinck | 03-0060 |
| Serva | 11924.03 |
| Sigma-Aldrich, St. Louis, MO, USA | B2261 |
| EMD Millipore | AB5539 |
| Merck, KGA, Darmstadt, Germany | D8418 |
| Merck, KGA, Darmstadt, Germany | AP194SA6 |
| Thermo Fisher Scientific | A11057 |
| Thermo Fisher Scientific | A21206 |
| Whatman (Sigma Aldrich) | WHA10310992 |
| Sigma Aldrich | E4009 |
| Th.Geyer | 2212.5000 |
| AppliChem | 253681.0008 |
| Southern Biotech | 0100-01 |
| Southern Biotech | 0100-20 |
| EMD Millipore | AP144P |
| Merck, KGA, Darmstadt, Germany | H1009 |
| Rotexmedica | PZN: 3862340 |
| Life technologies | 4368813 |
| Abbott Laboratories | 2594.00.00 |
| Merck | 1.09249.0500 |
| Sigma-Aldrich | 34860 |
| Marienfeld | 0101040 |
| Qiagen | 217004 |
| Thermo Fisher Scientific | ND-2000C |
| Akoya Bioscience | FP1488001KT |
| Alfa Aesar | 43368 |
| Th.Geyer | 7691202 |
| Gibco | 18912-014 |
| FineScienceTools | 11203-25 |
| Qiagen | 79306 |
| EMD Millipore | AB152 |
| Merck | R0901-100ML |
| biotechne (ACD) | 323100 |
| biotechne (ACD) | 431738-C2 |
| biotechne (ACD) | 423391 |
| Qiagen | 69990 |
| Roth | 0292.2 |
| Thermo Fisher Scientific | 4331182 |
| Thermo Fisher Scientific | 4331182 |
| Thermo Fisher Scientific | 4331182 |
| Thermo Fisher Scientific | 4331182 |
| Thermo Fisher Scientific | 4331182 |
| Thermo Fisher Scientific | 4331182 |
| Applied biosystems | 4370074 |
| Qiagen | 85300 |
| Sigma-Aldrich | 93443-100ml |
| Sigma-Aldrich | P9416-100ML |
| Wacom | CTL-460/K |
| Sigma-Aldrich | WHA10311647 |

**Comments/Description**

RNAscope
Microscopy
Whole mount staining
Whole mount staining
Whole mount staining
Whole mount staining
Whole mount staining
Whole mount staining
Whole mount staining
Whole mount staining
Whole mount staining
Whole mount staining
Whole mount staining
Whole mount staining
Whole mount staining
Whole mount staining
Preparation SG
RNA isolation
Preparation SG
Whole mount staining
Whole mount staining
Whole mount staining
RNA isolation
RNA isolation
RNAscope
Whole mount staining
Whole mount staining
Whole mount staining
Preparation SG
RNA isolation
Whole mount staining
RNA isolation (optional)
RNAscope
RNAscope
RNAscope
RNA isolation
Whole mount staining
Gene expression analysis
Gene expression analysis
Gene expression analysis
Gene expression analysis
Gene expression analysis
Gene expression analysis
Gene Expression analysis
RNA isolation
Whole mount staining
RNAscope
Cell size measurements
Whole mount staining

RNAscope

EVANGELISCHES KRANKENHAUS DÜSSELDORF

Akademisches Lehrkrankenhaus der Heinrich-Heine-Universität Düsseldorf

**Klinik für Kardiologie**

**Elektrophysiologie, Angiologie, Intensivmedizin**

**Chefarzt**
**Prof. Dr. med. Christian Meyer**

Kirchfeldstraße 40
40217 Düsseldorf

Sekretariat:
Frau Goebels / Frau Blaik
Telefon 02 11 / 9 19 – 18 55
Telefax 02 11 / 9 19 – 39 55
eMail kardiologie@evk-duesseldorf.de
Internet www.evk-duesseldorf.de

EVK Düsseldorf, Kardiologische Klinik, Postfach 10 22 54, 40013 Düsseldorf

To
Nam Nguyen, Ph.D.
Manager of Review
JoVE
nam.nguyen@jove.com

27 October 2020

Rebuttal: JoVE submission JoVE62026

Dear Dr Nam Nguyen, dear editorial board,

Thank you very much for the opportunity to submit a revised version of our manuscript.

We are grateful for the valuable and highly constructive feedback we received from the editors and reviewers. We are convinced that integration of the reviewers' comments and revision of the manuscript led to a considerable improvement in quality.

All comments and questions raised from the editors and reviewers are implemented in the revised version of the manuscript and are addressed the following point-by-point response. Changes in the manuscript are highlighted in green, while our suggestion for the video protocol are marked in yellow.

Yours sincerely,

Katharina Scherschel and Christian Meyer

Reviewer #1:

Manuscript Summary: Authors describe a method to collect and process left stellate ganglion in mice. The manuscript is interesting and useful, well written and extremely clear. All the parts are complete and easy-to-use for the researchers needing technical procedures. Authors are well focused on the scientific question and bibliography is exhaustive.

Major Concerns: there are no major concerns.

We thank reviewer 1 for his/her efforts and for agreeing that our manuscript is interesting and useful. All comments by this reviewer are now addressed in the following response and discussed in the manuscript as requested.

Minor Concerns:

Figure 1 is not enough clear for a surgeon new to the technique. My suggestion is to provide an additional figure with a schematic diagram, e.g. add a diagram drawn, made with power point or by freehand, highlighting the main anatomical points useful for orientation during dissection.

We thank reviewer 1 for this suggestion. The reviewer is right that the image was not clear enough. In response to this comment, we now included a schematic figure into the revised version of the manuscript which highlights the main anatomical points useful for orientation during dissection. Additionally, we have now included a new photographic description of the dissection to be clearer for a surgeon new to the technique.

*Figure 1*

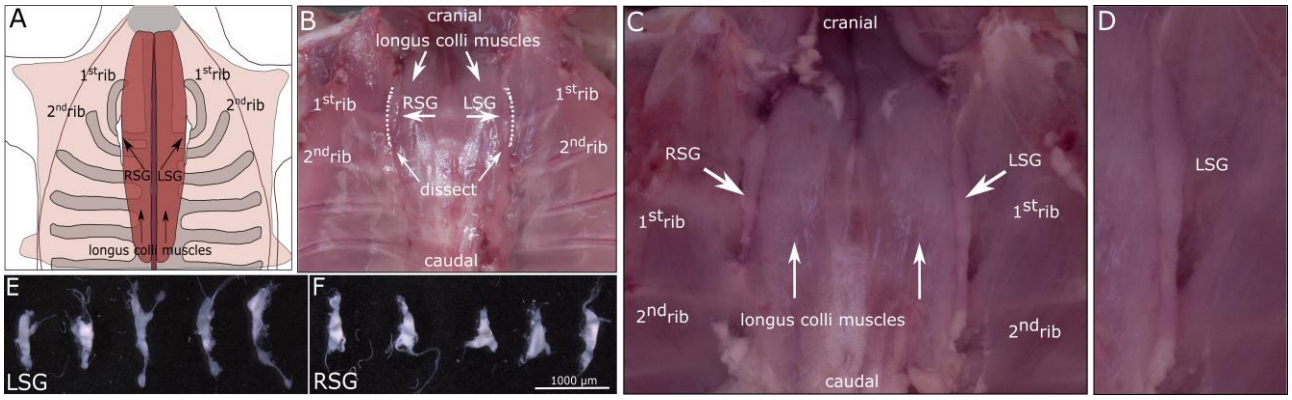


**Figure 1: Location, dissection and morphology of the murine stellate ganglia.** (A) Schematic drawing of the location of the stellate ganglia (SG). (B) View into the thorax after removal of the heart-lung package. It is important to note that the stellate ganglia are not immediately visible most of the time. The longus colli muscles are located lateral from the spine. The SG are located lateral from the muscles at the junction with the first rib. Carefully dissect lateral to the muscles (area marked by dotted line) to uncover the ganglia. After dissection, ganglia (left and right, LSG and RSG respectively) and the sympathetic chain can be made out as white, long structures. (C) An exemplary dissection showing the ganglia and anatomical landmarks. (D) Magnification of the left stellate ganglion. (E) LSG and (F) RSG from wild type, male C57Bl6 mice (16 weeks) were dissected and photographed to show the variations in morphology and size. Scale bar represents 1000 µm.

*Page 9, line 381, Representative Results*

**Figure 1** visualizes how to identify and dissect the SG. **Figure 1A** shows a schematic drawing of the location, while **Figure 1B** presents the view into the thorax after removal of the heart-lung-package. The left and right

longus colli muscles medial from the SG and the rib cage are important landmarks for orientation. Dissection is performed along the dotted lines between muscles and first rib. The SG and the sympathetic chain become visible as white structures (**Figure 1C**). **Figure 1D** shows a magnification of the region between the left longus colli muscle and the first rib, where the left SG is located. […]

**Authors are also encouraged to follow ARRIVE guidelines to provide all information needed in manuscripts describing animal procedures. The guidelines are available at: https://www.nc3rs.org.uk/arrive-guidelines**

We thank the reviewer for raising this important point. In consequence to this encouragement we carefully checked the ARRIVE guidelines and provide additional information to complement the previous version of the manuscript as recommended by this reviewer.

*Page 3, line 102 ff., Protocol*

[…] All procedures involving animals were approved were approved by the Animal Care and Use Committee of the State of Hamburg (ORG870, 959) and conform to the National Institutes of Health's Guide for the Care and Use of Laboratory Animals (2011). Studies were performed using male and female (aged 10-24 weeks) C57BL/6 mice (stock number 000664, Jackson Laboratories) and mice homozygous (db/db) or heterozygous (db/het; control) for the diabetes spontaneous mutation (Leprdb; BKS.Cg-Dock7$^{m+/+}$ Leprdb /J, stock number 000642, Jackson Laboratories). […]

*Page 10, line 430-431, Representative Results*

[…] Statistical significance was defined as a P value of <0.05, statistical analysis was performed using Graphpad Prism Version 6. […]

Reviewer #2:

Manuscript Summary:

The authors did a very good job of describing the methodology. The necessary details appear complete.

We thank Reviewer 2 for the positive feedback on our description of methodology and his/her helpful comments which we answer in the following.

Major Concerns:

The major concerns I have with the paper are the following:

1) Our laboratory routinely isolates rat SG neurons for electrophysiological studies. In our approach, we are able to remove the entire connective tissue from the SG. The authors suggest to readers that chemical dissolving may work but it did not work in the authors' hands. I would like to point out that removing the entire connective tissue is not a difficult thing to do. It is akin to removing one's socks. Alternatively, sharp forceps can be used to remove the connective tissue.

We thank the reviewer very much for raising this point and sharing his/her experiences with the isolation of rat SG neurons. As this is an important note, we now address this issue in the revised manuscript and added relevant literature. In addition, we outline that removal of the capsule might vary between species, the type of ganglion and age.

*Page 4, line 155 ff., Protocol: 1. Location and dissection of murine stellate ganglia*

Note: Autonomic ganglia are surrounded by a connective tissue capsule consisting of collagen fibres and fibroblasts [26, 27]. The permeability of these capsules seems to vary amongst species, different kind of ganglia [26] and age [28]. Remove as much connective tissue as possible using Dumont #5/45 forceps and, if necessary, spring scissors.

*Page 13, line 521 ff., Discussion*

[…] Some pitfalls should be kept in mind with the presented methods: we observed inconsistencies in antibody-based staining at some occasions and hypothesized that incomplete removal of the connective tissue capsule ensheathing the SG might be at fault, as they have been described to vary in permeability amongst different types of ganglia.[26] Mechanical removal of the capsule using fine forceps has been described in the superior cervical ganglion of rats up to postnatal day 10 [28] and desheathing is mentioned in literature for adult rat SG [54,55] and mice [56]. Removal of the SG capsule might vary between age [28] and – due to size differences – species. In our experience, fresh dissection, removal of as much connective tissue as possible using fine forceps and thorough permeabilization as described in the protocol at hand, are important factors for successful staining. […]

2) I think it is crucial that the authors inform the reader that SG innervate not only the heart, but they innervate the lungs and sweat glands. Therefore, in their paper, they should avoid making statements that with this approach one is able to study cardiac innervating SG neurons. Normally, the cardiac muscle is injected with a dye that will travel to the SG soma in a retrograded manner to identify cardiac muscle-innervating SG neurons. Unless the SG neurons are labeled, it can't be known with certainty what SG cell subtype is under study.

We thank the reviewer for raising this point. In consequence to this comment, we now inform the reader that the SG also innervates lungs and sweat glands and that it cannot be known with certainty what SG cellular subtype is under study.

*Page 13, line 505 ff., Discussion*

[…] It is important to note that the heart is not the only target of the SG. Amongst others, lungs [47] and sweat glands in the forepaw [48] are also innervated from fibres originating in the SG, the latter are an exception to sympathetic physiology as they express choline acetyltransferase [37]. […]

*Page 13, line 510 ff., Discussion*

[…] When focussing on cardiac disease models, it should be kept in mind for interpretation of results that cardiac neurons cannot be differentiated by morphology or electrophysiological properties from non-cardiac neurons [51]. This can be achieved by retrograde tracing, thereby the location of neurons projecting to the heart was shown to be located in the cranio-medial parts of the SG[52]. […]

**3) Another important fact that authors should point out is that the SG neurons that innervate sweat glands are a unique exception in sympathetic physiology. That is, the main neurotransmitter released is acetylcholine, and these SG neurons are, thus, cholinergic. This further implies that this neuron subtype expresses choline acetyltransferase. Therefore, how did the authors distinguish between Chat expressed in ICN versus SG neurons innervating sweat glands?**

We thank the reviewer for this remark. In consequence, we now point out in the revised manuscript that innervation of sweat glands from the SG is an exception in sympathetic physiology in regard to release of acetylcholine as main neurotransmitter.

*Page 13, line 505 ff., Discussion*

Amongst others, lungs [47] and sweat glands in the forepaw [48] are also innervated from fibres originating in the SG, the latter are an exception to sympathetic physiology as they express choline acetyltransferase [37].

We did not distinguish between *Chat* expressed in ICN and SG neurons on RNA level, but as reviewers 3 and 4 pointed out, fibers in the SG immunoreactive for ChAT on protein level are most likely preganglionic (Morales et al. Proc. Natl. Acad. Sci. USA, 1995, Jiminez et al., Synpase, 2002). Neuronal somata expressing ChAT can thus be accounted to SG neurons innervating sweat glands. In consequence to this comment, we removed the comparison of *Chat* mRNA in ICN versus SG from the revised manuscript to avoid confusion.

**4) In regard to Section 5 (Molecular Analyses), the authors should also point out that the gene expression profile the experimenter will obtain will be made up of glial cells and SG neurons innervating heart, lungs and sweat glands. Therefore, any conclusions drawn from the results with this approach should be done with caution.**

We thank the reviewer for pointing this out. To address this issue appropriately, we have now included new data into the revised manuscript pointing out for the experimenter that the gene expression profile will be made up from glial cells as well as neurons.

The revised version of the manuscript now includes an updated Figure 2 (changes in the Figure are marked with a red box below) with a double in situ hybridization presenting *S100b* (as glial marker) and *Tubb3* mRNA (as neuronal marker) co-stained with an antibody targeting tyrosine hydroxylase showing different kinds of neurons and glial cells.

Additionally, we have included gene expression data of *S100b*, but also *Ki67* as a marker for proliferating cells in Figure 3.

Last, we noted in the discussion that the SG consists of different kinds of cells.

*Page 10, line 400 ff., Representative Results*

[…] Figure 2C-F show exemplary analyses to study the SG on a subcellular level, using whole mount in situ hybridization and immunofluorescent co-staining. The protein TH (Figure 2C, red) and mRNA molecules of *Tubb3* (Figure 2D, white) are expressed in large neuronal cell bodies, while mRNA of *S100b* (Figure 2E, green) is also detectable in surrounding glia cells. In the merge (Figure 2F), it is visible that some neurons are negative for TH but express *Tubb3*, while *S100b* mRNAs can also be detected in surrounding cells, as depicted in the magnification in Figure 2G. […]

*Figure 2*

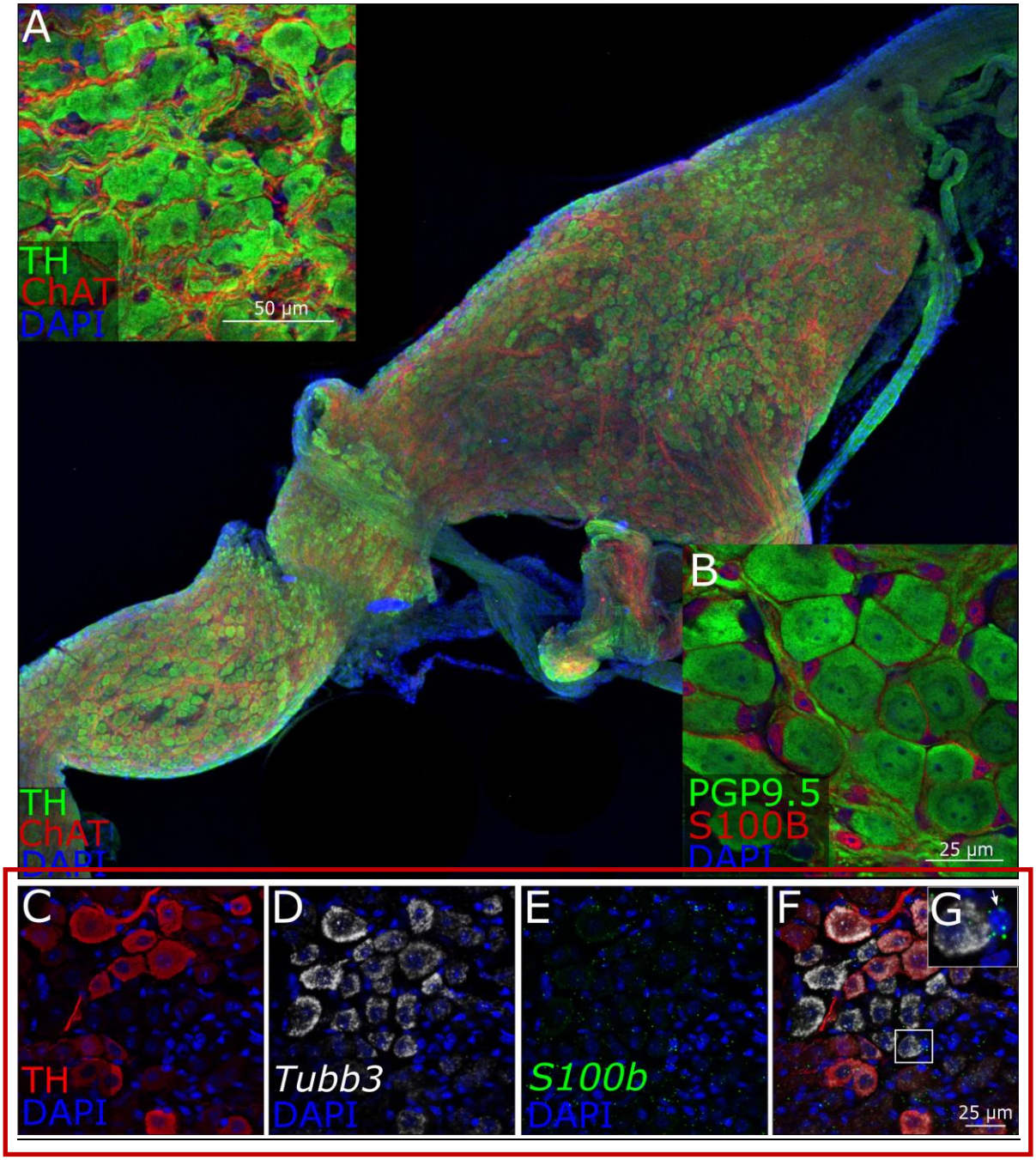

**Figure 2: Visualization of different cell types in murine stellate ganglia via whole mount immunohistochemistry and in situ hybridization.** (A) Gross overview of a murine stellate ganglion stained for the sympathetic marker tyrosine hydroxylase (TH) and choline acetyltransferase (ChAT). The magnification shows strongly TH-positive cell bodies and the presence of ChAT-positive, most likely presynaptic, nerve fibers surrounding neuronal somata. (B) Glial cells ensheathing neuronal cell bodies can be visualized by staining for S100B, here in combination with the neuronal marker PGP9.5 (C-F) Microscopic images from one SG stained whole mount via a combination of immunohistochemistry for TH (red) and in situ hybridization for *Tubb3* (D, white) and *S100b* (E, green). Nuclei are counterstained with DAPI (blue). (F) The merge shows that not all neuronal (*Tubb3*-positive) cells are TH positive. *S100b* mRNAs can be detected within neuronal somata, but also surrounding cells, as marked by an arrow in the magnification in (G).

*Figure 3C*

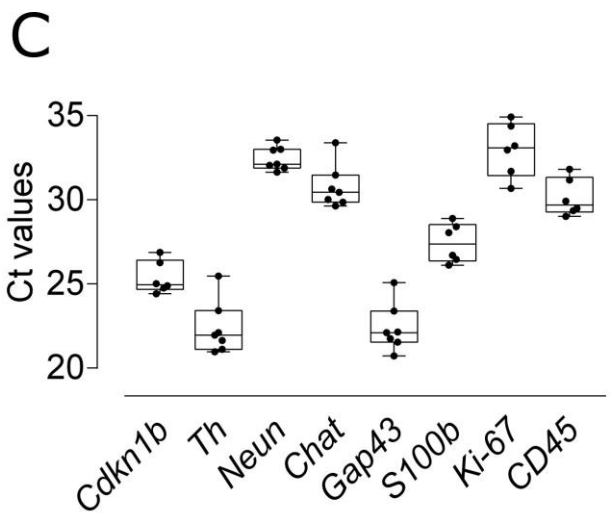


**Figure 3: Potential quantitative analyses and pitfalls**. […] (C) Exemplary genes expressed in the SG that might be useful for characterizing molecular processes. *Cdkn1b* as well as the neuronal marker *Neun/Rbfox3* (to account for the presence of other cell types) can be used for normalization. Tyrosine hydroxylase (*Th*) serves as a sympathetic marker, choline acetyltransferase (*Chat*) for cholinergic transdifferentiation, *Gap43* for neuronal sprouting. Genes expressed in non-neuronal cell types include *S100b* (glial cells), *Ki-67* (proliferating cells) and *Cd45* (immune cells).

*Page 10, line 412 ff., Representative results*

**Figure 3C** shows the expression of genes from different cell types of the SG (n = 6-7). Pooling of both SG from one animal allows gene expression measurements of approximately 24 assays (12 genes in duplicates). We typically normalize samples for *Cdkn1b* (detected at Ct values of 25.4 ± 0.97) as well as the neuronal marker *Neun/Rbfox3* (32.5 ± 0.7) if it is necessary to account for other cell types and neuronal purity of the dissection. Genes that we found useful for characterizing molecular processes in the SG include the sympathetic gene *Th* (22.4 ± 1.6), *Chat*, which could indicate cholinergic transdifferentiation (detectable at Ct values of 30.8 ± 1.3) and *Gap43*, a marker for neuronal sprouting (22.4 ± 1.4). Genes expressed in non-neuronal cell types include *S100b* (for glial cells, 27.3 ± 1.2), *Ki-67* (for proliferating cells, 33.0 ± 1.6) and *Cd45* (for immune cells, 30.2 ± 1.1).

*Page 13, line 515 ff., Discussion*

*[…]* Additionally, it is important to note that besides different types of neurons, sympathetic ganglia are made up of ensheathing glia, so-called satellite glial cells or satellite cells, marked by expression of the glial

marker S100B [53]. While little is known about the role of these cells in cardiovascular pathologies, glial activation and expression of the glial fibrillary acidic protein (GFAP) has been described in SG from patients with arrhythmias [18]. […]

Minor Concerns:

Line 127: "rip" should be "rib"

Thank you, we have corrected this in the revised manuscript.

Line 84: please explain what "IIb" refers to.

We thank the reviewer for this remark. As this was also mentioned by reviewer 4, we now see that guideline-specific language for clinical recommendations is confusing for the target audience. In consequence, we have now excluded this from the revised version of the manuscript.

*Page 2, line 84 ff., Introduction*

[…] Cardiac sympathetic denervation presents an option for patients with therapy-refractory VA with promising results [14, 16, 17]. […]

Reviewer #3:

This very useful piece provides a thorough description of identifying and removing stellate ganglia from mice. The photos included are extremely helpful. This work will be a great training resource for people trying to study SG in mouse models of cardiovascular disease. I have no concerns, just a few minor edits to suggest.

We thank reviewer 3 for this positive appreciation of our work and for agreeing that this will be a great training resource. We answer the minor suggestions by this reviewer in the following.

Line 92. It looks like words are missing after the word "via"

We thank the reviewer for finding this editing mistake. The sentence is now corrected.

*Page 3, line 90 ff., Introduction*

*[…] Experimental studies present novel approaches to treat VA, for example the reduction of sympathetic nerve activity via optogenetics,[22] but in-depth characterization of the SG is still lacking in many cardiac pathologies that go in hand with VA. […]*

Line 127. Last word should be rib instead of rip

Thank you, we have now corrected this in the revised manuscript.

Line 305 section 5.1 - Please consider adding the option that ganglia can be placed in RNAlater on ice if freezing immediately is not an option.

We thank the reviewer for suggesting this option. Our lab has no experiences with RNAlater for the isolation of RNA from SG, but in consequence of this comment, we have now included this as an option for the experimenter in the revised protocol and Table of Materials.

*Page 9, line 341 ff., Protocol*

[…] have liquid nitrogen ready for shock-frosting or consider commercial solutions for protection of RNA (optional, see Table of Materials) [36].

Line 342 suggested edit: "A certain amount of para pre-ganglionic sympathetic fibers is are detectable". These ChAT immunoreactive fibers are probably mostly pre-ganglionic sympathetic fibers.

We thank the reviewer for raising this important point. In consequence of this comment, we have now included the fact that ChAT immunoreactive fibers are probably mostly pre-ganglionic sympathetic fibers in the revised version of the manuscript.

*Page 10, line 395 ff., Representative Results*

[…] TH-expressing neuronal somata are surrounded by nerve fibers staining positive for choline acetyltransferase (ChAT). These are most likely presynaptic fibers [37, 38]. […]

*Page 11, line 448 ff., Figure 2 Subtitle*

[…] Gross overview of a murine stellate ganglion stained for the sympathetic marker tyrosine hydroxylase (TH) and choline acetyltransferase (ChAT). The magnification shows strongly TH-positive cell bodies and the presence of ChAT-positive, most likely presynaptic, nerve fibers surrounding neuronal somata. […]

Reviewer #4:

Manuscript Summary: This methods article describes protocols for the location, dissection, and characterisation of the murine stellate ganglion (SG) at the RNA, protein, and cellular level. The SG contains sympathetic neurons that innervate the heart, and is therefore an important target for the treatment of ventricular arrhythmias. The existence of a video protocol describing the location and dissection of murine SG will be extremely useful for the scientific community, and have a positive general impact. As stated in the article, often the superior cervical ganglion is used instead of the SG to study the sympathetic innervation of the heart in mice, because many researchers do not know how to dissect the SG. Furthermore, the other protocols presented contain useful practical tips on how to characterise the SG and information on how to optimise these techniques for SG neurons.

General comments: The efficacy of the protocol is demonstrated by the experimental results shown in the figures. The clarity of presentation is good. This article is compliant with research standards and has a good technical quality and efficiency. The protocols in this article are detailed and thorough enough such that a researcher in the field could replicate the experiment, except for the protocol for the location and dissection of the SG. This protocol would greatly benefit from the video format. The abstract is appropriate for this methods article. I expect that the steps listed in the procedure would lead to the described outcome. They are clearly explained, and there are no important steps missing. Critical steps are highlighted. The included examples of ways to characterise the SG will be useful to readers.

We thank reviewer 4 for his/her constructive and extensive feedback. We appreciate the time and efforts invested by this reviewer and are convinced that integration of this feedback led to a considerable improvement of the manuscript.

Major Concerns:

Scientific inaccuracy on lines 342 and 375: These ChAT positive fibres are not parasympathetic nerve fibres. These are more likely to be presynaptic sympathetic fibres.

We thank the reviewer for pointing this out. Please excuse. In consequence, we have now corrected in the revised version of the manuscript that ChAT immunoreactive fibers are most likely pre-ganglionic sympathetic fibers and added appropriate citations.

*Page 10, line 395 ff., Representative Results*

[…] TH-expressing neuronal somata are surrounded by nerve fibers staining positive for choline acetyltransferase (ChAT). These are most likely presynaptic fibers [37, 38]. […]

*Page 11, line 450 ff., Figure 2 Subtitle*

[…] (B) The magnification shows sympathetic, strongly TH-positive cell bodies and the presence of presynaptic, ChAT-positive nerve fibers surrounding neuronal somata. […]

Minor Concerns:

The title is not descriptive enough.

We thank the reviewer raising this concern. We have now changed the title of the manuscript to be more descriptive.

*Title:* “The murine stellate ganglion - location, dissection and analysis”

Appropriate controls should be suggested in the protocols.

Thank you for noting this. In consequence of this comment, we now suggest appropriate technical controls at several steps in the protocols.

*Page 5, line 207 ff., Protocol*

Note: Include one SG as antibody control without primary antibody (incubated with antigen-preabsorbed antibody or IgG if available, or blocking buffer).

*Page 7, line 272 ff., Protocol*

Note: Include one SG as negative control, using a probe against a bacterial gene (e.g., dihydro-dipicolinate reductase, Dapb), to check for unspecific binding of amplification reagents in later steps.

*Page 9, line 335 ff., Protocol*

Note: Include controls depending on your experimental design. This could be SGs with different genotypes and disease background and/or other autonomic ganglia, such as the sympathetic superior cervical ganglion (located in the neck area, see detailed description in Ziegler et al. [35]) or parasympathetic ganglia (such as intracardiac ganglia, see Jungen et al.[4]).

*Page 9, line 360 ff., Protocol*

Note: To exclude contamination of the purified RNA with genomic DNA we propose performing a polymerase chain reaction with genomic primers and 1 µl RNA as template, instead minus reverse transcriptase control. This will safe a significant amount of RNA. If RNA is contaminated, use exon-intron boundary primers or intron flanking primers for subsequent quantitative real time polymerase chain reaction.

*Page 9, line 374 ff., Protocol*

Note: Perform non-template control for every gene to exclude false positive results.

The SG is not just involved in cardiac electrophysiology. Other potential applications for the protocols in this **article should be included.**

We thank the reviewer for this important remark. To address it, we have included other potential applications for this protocol in the article.

*Page 13, line 505 ff., Discussion*

[…] It is important to note that the heart is not the only target of the SG. Amongst others, lungs [47] and sweat glands in the forepaw [48] are also innervated from fibres originating in the SG, the latter are an exception to sympathetic physiology as they express choline acetyltransferase [37]. Temporary blockade of the SG is studied with regard to inflammatory processes in acute lung injury [49] or for treatment of hot flushes and sleep dysfunction [50], therefore the protocols at hand might offer a repertoire for mechanistic questions in these fields. […]

**It would be useful** to include additional information about the size and shape of the SG. Can the experimenter expect the SG to vary in size and shape between animals of the same sex and age, and between right and left SG?

We thank the reviewer for this question and fully agree that this will be useful information for the experimenter. Therefore, in consequence for this comment, we have now included new data about the size and shape of the SG.

*Figure 1D, E*

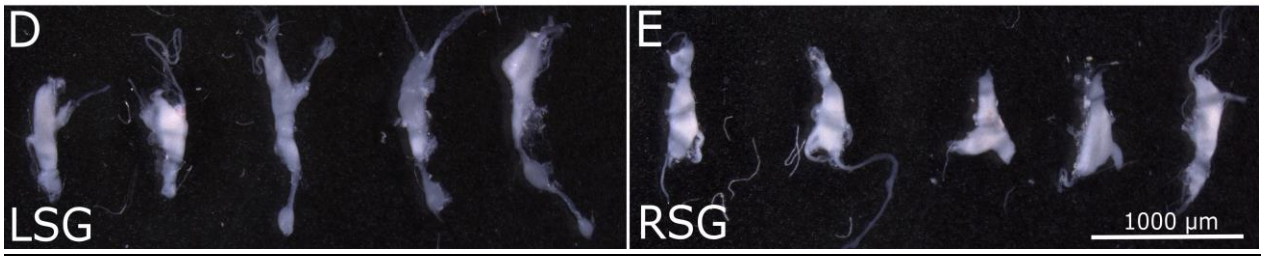


**Figure 1: Location, dissection and morphology of the murine stellate ganglia.** […] (D) LSG and (E) RSG from wild type, male C57Bl6 mice (16 weeks) were dissected and photographed to show the variations in morphology and size. Scale bar represents 1000 µm.

*Page 10, line 387 ff., Representative Results*

Morphology of the stellate ganglion differs between individuals. It often consists of a fusion of the inferior cervical and the first to the third thoracic ganglia [24]. Some variety that the experimenter can expect in murine SG is depicted in **Figure 1D and E**, where left and right SG of 5 male C57Bl6 wild type mice are photographed.

The materials and equipment table contains unnecessary German text (e.g. "vergällt mit" and "graduiert"). This table also contains irregular fonts.

We thank the reviewer for this thorough evaluation and excuse for the negligence. In consequence of this comment, we have carefully revised the materials and equipment table.

Previously published protocols are not cited properly for:

- "The location and dissection of murine stellate ganglia." There are some previously published descriptions of this method, albeit less detailed.

We thank the reviewer for pointing this out. In consequence to this comment we have now included citations of previously published protocols. In case we have accidentally omitted an important citation, we are grateful to learn about and include it in our revised manuscript.

*Page 3, line 112 ff., Protocol Step 1*

Note: Even though descriptions and drawings are mostly available in bigger species, some publications have previously described location of the SG in rats [24] and mice [25] using anatomical methods and fluorescent reporter lines, respectively.

- "Whole mount immunohistochemistry protocol." Please include a sentence at the start of section 2, with a reference to the protocol(s) this is based on.

We thank the reviewer for finding these flaws. We now include proper citations of the protocols this is based on.

*Page 4, line 163., Protocol*

[…] This protocol is adapted from cardiac whole mount stainings [4, 29].[…]

84: "With a IIb recommendation". This clinical jargon may be unfamiliar to the target audience.

We thank the reviewer for this remark. Thanks to this and to the question by reviewer 2, we now see that guideline-specific language for clinical recommendations is confusing for the target audience. In consequence, we have now excluded this jargon from the revised version of the manuscript.

*Page 2, line 84 ff., Introduction*

[…] Cardiac sympathetic denervation presents an option for patients with therapy-refractory VA with promising results [14, 16, 17]. […]

92: "reduction of sympathetic nerve activity, via ..., but in-depth characterization". Part of sentence missing.

We thank the reviewer for finding this editing mistake and have changed it accordingly.

*Page 3, line 90 ff., Introduction*

[…] Experimental studies present novel approaches to treat VA, for example the reduction of sympathetic nerve activity via optogenetics [22], but in-depth characterization of the SG is still lacking in many cardiac pathologies that go in hand with VA. […]

110: "Euthanize mouse". At what age range can this dissection be performed? Can you suggest any variations to the protocol for dissection of very young/old mice?

We thank the reviewer for this question. In consequence to this question and the remark by reviewer 1, we have now included age of the mice used in this study.

While we do not have experiences with mice younger than this age range, we have performed SG dissection in mice up to 60 weeks with this protocol. This is now included as a remark in the protocol.

*Page 3, line 104 ff., Protocol*

[…] Studies were performed using male and female (aged 10-24 weeks) C57BL/6 mice (stock number 000664, Jackson Laboratories) and mice homozygous (db/db) or heterozygous (db/het; control) for the diabetes spontaneous mutation (Leprdb; BKS.Cg-Dock7m+/+ Leprdb /J, stock number 000642, Jackson Laboratories). The authors have used the protocols at hand without variations for mice aged up to 60 weeks. […]

112: "in ripping off". Informal language.

Thank you, we removed informal language from the revised protocol.

*Page 3, line 122 ff., Protocol*

[…] Incorrect cervical dislocation can result in (1) breakage of the spine and damage of thoracic vessels leading to bleeding which hinders preparation or (2) in severing the sympathetic chain, so that SG are not in their correct position. […]

135: "Turn the forceps around by 180 °C" - remove C.

Thank you, we removed "C" from the revised protocol.

365: Fig1A/B. The absence of color in this image makes it much harder to identify different tissues. Please include a color image of your dissection.

We appreciate the feedback on the image in Figure 1A/B and agree that it might be hard to identify different tissues. In consequence to the suggestion by this reviewer, we have now revised Figure 1 and included new images of our dissection in color. Additionally, we have included a schematic drawing according to the suggestion of reviewer 1.

*Figure 1*

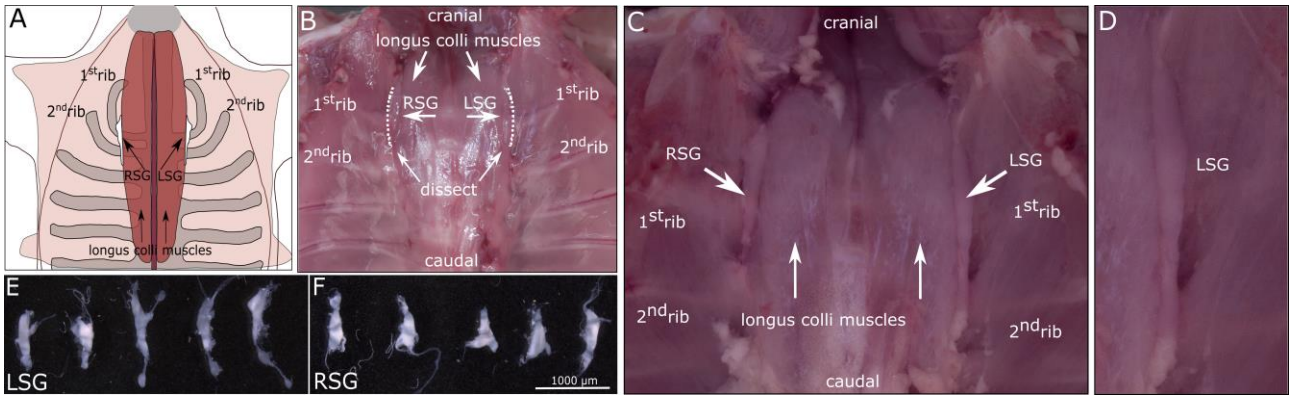


**Figure 1: Location, dissection and morphology of the murine stellate ganglia.** (A) Schematic drawing of the location of the stellate ganglia (SG). (B) View into the thorax after removal of the heart-lung package. It is important to note that the stellate ganglia are not immediately visible most of the time. The longus colli muscles are located lateral from the spine. The SG are located lateral from the muscles at the junction with the first rib. Carefully dissect lateral to the muscles (area marked by dotted line) to uncover the ganglia. After dissection, ganglia (left and right, LSG and RSG respectively) and the sympathetic chain can be made out as white, long structures. (C) An exemplary dissection showing the ganglia and anatomical landmarks. (D) Magnification of the LSG. (E) LSG and (F) RSG from wild type, male C57Bl6 mice (16 weeks) were dissected and photographed to show the variations in morphology and size. Scale bar represents 1000 µm.

*Page 10, line 381, Representative Results*

**Figure 1** visualizes how to identify and dissect the SG. **Figure 1A** shows a schematic drawing of the location, while **Figure 1B** presents the view into the thorax after removal of the heart-lung-package. The left and right longus colli muscles medial from the SG and the rib cage are important landmarks for orientation. Dissection is performed along the dotted lines between muscles and first rib. The SG and the sympathetic chain be-

come visible as white structures (Figure 1C). Figure 1D shows a magnification of the region between the left longus colli muscle and the first rib, where the left SG is located. […]

Fig 3: It is unclear how intracardiac neurons were obtained. Please include methods. It is unclear why SG neurons are compared to intracardiac neurons. Please clarify, or use a comparison to other ganglion neurons instead, such as from the SCG or parasympathetic ganglia.

We thank the reviewer for this feedback. The revised version of the manuscript now clarifies how to obtain SCG or parasympathetic ganglia as controls. As detailed methods for dissection of other ganglia was beyond the scope of this protocol, we have included recommendations and important key references.

*Page 9, line 335, Protocol*

Note: Include controls depending on your experimental design. This could be SGs with different genotypes and disease background and/or other autonomic ganglia, such as the sympathetic superior cervical ganglion (located in the neck area, see detailed description in Ziegler et al. [35]) or parasympathetic ganglia (such as intracardiac ganglia, see Jungen et al.[4]).

Fig legend of 3B should include statistical test used.

Thank you for finding this flaw. We have now included Mann-Whitney test as the statistical test used in Figure 3B.

*Page 11-12, line 460 ff., Figure legend*

[…] (B) This was performed in a mouse model of diabetes (100 cells per SG, n = 2 SG per genotype, data were compared using Mann-Whitney test). […]

Fig 3C is a comparison between fibres in the SG and cell bodies of ICN, therefore this is not an informative comparison. The SG does contain a very small percentage of cholinergic neuron cell bodies (<5%), which innervate the sweat glands in the forepaws, but most of the ChAT found in the SG is contained within the presynaptic sympathetic fibres. Please provide a rationale for this comparison, or compare SG to a different ganglion instead.

We thank the reviewer for this point. We agree that this comparison is not useful. Therefore, in consequence of this comment, we now state that the SG contains cholinergic neuronal cell bodies innervating the sweat glands in the forepaws, that cholinergic fibers in the SG are presynaptic sympathetic fibers and excluded the comparison with intracardiac neurons and replaced it with a panel of genes expressed in stellate ganglia.

*Page 13, line 505 ff., Discussion*

[…] It is important to note that the heart is not the only target of the SG. Amongst others, lungs [47] and sweat glands in the forepaw [48] are also innervated from fibres originating in the SG, the latter are an exception to sympathetic physiology as they express choline acetyltransferase [37]. […]

*Page 10, line 395 ff., Representative Results*

[…] TH-expressing neuronal somata are surrounded by nerve fibers staining positive for choline acetyltransferase (ChAT). These are most likely presynaptic fibers [37, 38]. […]

*Page 11, line 450 ff., Figure 2 Subtitle*

[…] (B) The magnification shows sympathetic, strongly TH-positive cell bodies and the presence of presynaptic, ChAT-positive nerve fibers surrounding neuronal somata. […]

*Figure 3C*

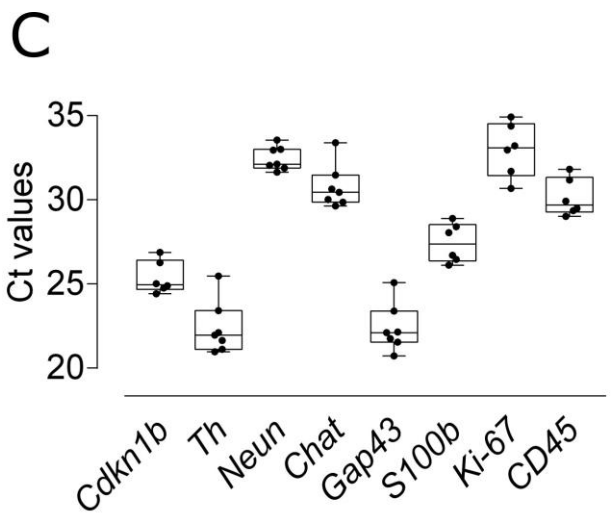


**Figure 3: Potential quantitative analyses and pitfalls**. […] (C) Exemplary genes expressed in the SG that might be useful for characterizing molecular processes. *Cdkn1b* as well as the neuronal marker *Neun/Rbfox3* (to account for the presence of other cell types) can be used for normalization. Tyrosine hydroxylase (*Th*) serves as a sympathetic marker, choline acetyltransferase (*Chat*) for cholinergic transdifferentiation, *Gap43* for neuronal sprouting. Genes expressed in non-neuronal cell types include *S100b* (glial cells), *Ki-67* (proliferating cells) and *Cd45* (immune cells).

*Page 10, line 413 ff., Representative results*

Figure 3C shows the expression of genes from different cell types of the SG (n = 6-7). Pooling of both SG from one animal allows gene expression measurements of approximately 24 assays (12 genes in duplicates). We typically normalize samples for *Cdkn1b* (detected at Ct values of 25.4 ± 0.97) as well as the neuronal marker *Neun/Rbfox3* (32.5 ± 0.7) if it is necessary to account for other cell types and neuronal purity of the dissection. Genes that we found useful for characterizing molecular processes in the SG include the sympathetic gene *Th* (22.4 ± 1.6), *Chat*, which could indicate cholinergic transdifferentiation (expressed at Ct values of 30.8 ± 1.3) and *Gap43*, a marker for neuronal sprouting (detectable at Ct values of 22.4 ± 1.4). Genes expressed in non-neuronal cell type include *S100b* (for glial cells, 27.3 ± 1.2), *Ki-67* (for proliferating cells, 33.0 ± 1.6) and *Cd45* (for immune cells, 30.2 ± 1.1).

Fig. 3F is unclear. What is the dark blue stain? Which side of the dotted line shows failed staining? Which characteristic can be used to identify this as failed staining? How does this image show that fat and connective tissue prevent proper staining here?

We thank the reviewer for his opinion on Figure 3F. In consequence to this comment, we have now included a different staining of the same specimen and clearly state that the dark blue stain is DAPI. We clarify anti-

bodies do only show a clear signal in some parts of the staining, even though DAPI shows that cells are present.

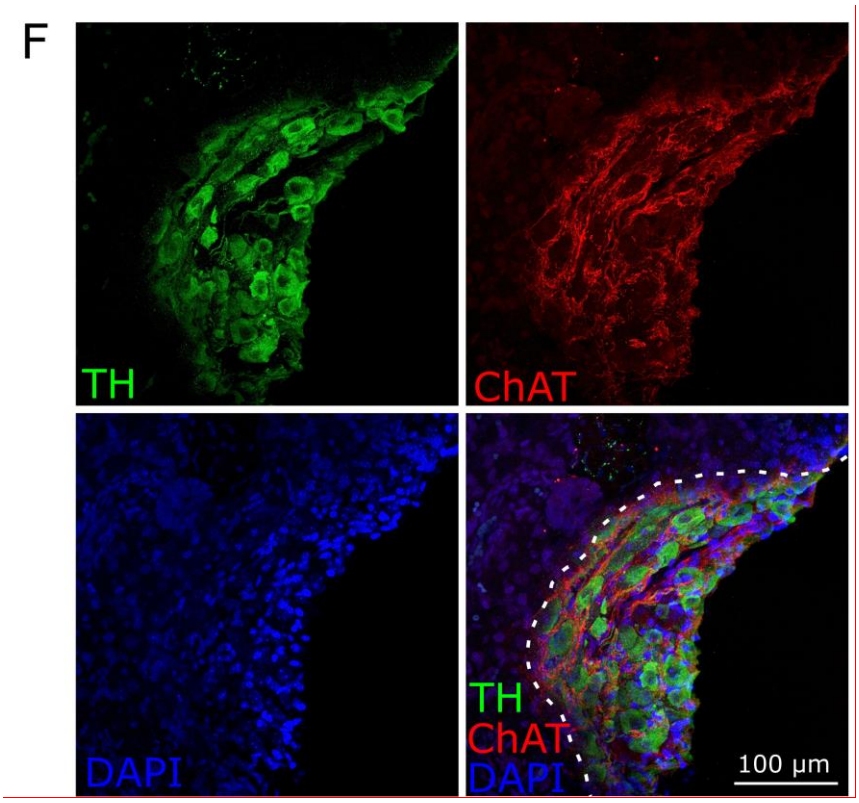


**Figure 3: Potential quantitative analyses and pitfalls.** […] (F) At some occasions we observed failure in antibody-based staining, most likely due to incomplete removal of the capsule. While ChAT (red) and TH (green) staining are only detectable in some parts of the SG, nuclei counterstained with DAPI (dark blue) are detectable throughout. The dotted line in the merged image separates successful staining (right of the line) from un-successful staining (left of the line).

*Page 11, line 423 ff., Representative results*

The SG is surrounded by a capsule of connective tissue [26], visualized via hematoxylin and eosin staining in **Figure 3D and E**. Occasionally, we observed inconsistencies in antibody-based staining as demonstrated in **Figure 3F**. While ChAT and TH staining are only detectable in some parts of the SG, nuclei counterstained with DAPI are detectable throughout. The dotted line in the merged image separates successful staining (right of the line) from unsuccessful staining (left of the line).

383: please clarify that the model of diabetes referred to here is db/db mice.

Please excuse for being unclear. We now clarify in the revised results section that the mouse model used here is the common type II diabetes model db/db.

*Page 3, line 104 ff., Protocol*

[…] Studies were performed using male and female (aged 10-24 weeks) C57BL/6 mice (stock number 000664, Jackson Laboratories) and mice homozygous (db/db) or heterozygous (db/het; control) for the diabetes spontaneous mutation (Leprdb; BKS.Cg-Dock7m+/+ Leprdb /J, stock number 000642, Jackson Laboratories). […]

410: "Due to its small size, manipulation of the murine SG in vivo is challenging." Should include mention of the location of the SG compared to the SCG as well. The SCG is much more accessible in vivo in mice.

We thank the reviewer for this suggestion. We have now mentioned that the SG is located within the thoracic cavity, while the SCG is location more assessable in the neck.

*Page 12, line 491 ff., Discussion*

Due to its small size and its location within the thoracic cavity [24], manipulation of the murine SG in vivo is challenging, although it has been performed successfully [23]. Still, for this reason, some studies focus on the superior cervical ganglia, which are located more accessible in the neck, upstream of the SG in the sympathetic chain behind the carotid bifurcation into internal and external carotid arteries [24, 35].

423: The statement "Chemical dissolving and permeabilization of connective tissue did not work successfully in our hands." is too vague. Need to specify methods used and explain what "did not work successfully" means.

We thank the reviewer for raising this point. We agree with the reviewer that this description is vague as it is rather anecdotal from establishment of the protocol. Therefore, in consequence of this remark, we have removed vague parts, and added relevant literature on this topic.

*Page 13, line 521 ff., Discussion*

[…] Some pitfalls should be kept in mind with the presented methods: we observed inconsistencies in antibody-based staining at some occasions and hypothesized that incomplete removal of the connective tissue capsule ensheathing the SG might be at fault, as they have been described to vary in permeability amongst different types of ganglia.[26] Mechanical removal of the capsule using fine forceps has been described in the superior cervical ganglion of rats up to postnatal day 10 [28] and desheathing is mentioned in literature for adult rat SG [54, 55] and mice [56]. Removal of the SG capsule might vary between age [28] and – due to size differences – species. In our experience, fresh dissection, removal of as much connective tissue as possible using fine forceps and thorough permeabilization as described in the protocol at hand, are important factors for successful staining. […]